Palaeogeography, Palaeoclimatology, Palaeoecology 386 (2013) 415–435

Contents lists available at SciVerse ScienceDirect

Palaeogeography, Palaeoclimatology, Palaeoecology

journal homepage: www.elsevier.com/locate/palaeo

The drift history of Adria and Africa from 280 Ma to Present, Jurassic true polar wander, and zonal climate control on Tethyan sedimentary facies

G. Muttoni [a,b,*], E. Dallanave [c], J.E.T. Channell [d]

[a] Dipartimento di Scienze della Terra "A. Desio", Università degli Studi di Milano, via Mangiagalli 34, 20133 Milano, Italy
[b] ALP — Alpine Laboratory of Paleomagnetism, via Madonna dei Boschi 76, I-12016 Peveragno (CN), Italy
[c] Department of Earth and Environmental Science, Ludwig-Maximilians University, Munich D-80333, Germany
[d] Department of Geological Sciences, University of Florida, Gainesville, FL 32611, USA

ARTICLE INFO

Article history:
Received 25 February 2013
Received in revised form 7 June 2013
Accepted 10 June 2013
Available online 18 June 2013

Keywords:
Paleomagnetism
Adria
Africa
Apparent polar wander path
True polar wander
Jurassic
Zonal climate
Tethys
Sedimentary facies

ABSTRACT

The orogenic belts surrounding the undeformed Adriatic Sea represent the margins of an area known as *Adria*, the African promontory. We have undertaken a critical appraisal of paleomagnetic data from regions of Adria considered parautochthonous relative to Africa, obtained either from biostratigraphically dated sedimentary rocks, corrected for inclination shallowing, or from igneous rocks that are regarded as free from any inclination shallowing bias. Paleomagnetic directions were used to calculate paleomagnetic poles for comparison with coeval, and inclination flattening-free, paleomagnetic poles from stable Africa. Visual coherence of paleopoles for several time slices from the Early Permian to the Eocene supports the construction of a composite apparent polar wander path (APWP) valid for parautochthonous Adria and stable Africa. This composite APWP is compared to previous APWPs, finding good agreement with the global APWP of Kent and Irving (2010). Both APWPs show a remarkable and rapid polar shift of ~40° in the Jurassic that other APWPs tend to underestimate. We interpret this shift to represent a major episode of true polar wander (TPW), from ~183 Ma in the Early Jurassic to ~151 Ma in the Late Jurassic. Using a simple zonal climate model, the drift motion of Adria attached to Africa appears to be consistent with the distribution of Permian–Cretaceous sedimentary facies on Adria.

1. Introduction

The evolution of the Alpine orogeny and Atlantic spreading history (e.g., Dewey et al., 1989) and the debated paleogeographic evolution of Pangea in the Permian (Muttoni et al., 2003; Domeier et al., 2011a; Aubele et al., 2012) are intimately connected with the interpretation of Adria — the paleogeographic unit composed of the Adriatic foreland and surrounding fold-and-thrust belts (Fig. 1A) — as a promontory of the African plate (Channell et al., 1979; Channell, 1996; Rosenbaum et al., 2004). After several decades of extensive paleomagnetic research, we assert that even opponents (e.g., Màrton et al., 2010) of the Adria–Africa coherence hypothesis would not deny that the general distribution of Permian–Cenozoic paleomagnetic poles from parautochthonous regions of Adria (see below) show a strong African affinity (Channell, 1996; Satolli et al., 2007, 2008). Given the far-reaching consequences of the Adria–Africa connection, however, it is important to re-evaluate the paleomagnetic database of Adria as a proxy for the drift history of Africa. We performed a thorough literature review of paleomagnetic data from Adria to compare with coeval data from Africa. Data from Adria have been obtained from well-dated sedimentary rocks and have been corrected for inclination shallowing, or from igneous rocks assumed free from inclination shallowing. Paleomagnetic data from Africa are mainly from igneous rocks. We find significant coherence of Adria and Africa paleomagnetic poles through the Permian–Cenozoic, and use this coherence to support a major, rapid, and previously underestimated event of polar wandering in the Jurassic, recently described by Kent and Irving (2010), as well as to explain the deposition of several paleolatitude-dependent sedimentary facies in the Tethys Ocean during the Permian–Cretaceous.

2. Adria, the African promontory

Adria is the term applied to the largely undeformed Po–Adriatic foreland basin rimmed by three post-Late Jurassic orogens, the Alps, the Apennines, and the Dinarides (Channell et al., 1979), and bounded by the Tyrrhenian Sea in the west and the Ionian Sea (Speranza et al., 2012) in the southeast (Fig. 1A). Due to this complexity, it took decades to realize and accept the 'enigmatic' (Channell, 1996) close concordance of Permian and Mesozoic paleomagnetic poles from Adria and Africa, suggestive of substantial tectonic coherence between the two lithospheric units (Channell, 1996). Through extensive research conducted

* Corresponding author at: Dipartimento di Scienze della Terra "A. Desio", Università degli Studi di Milano, via Mangiagalli 34, 20133 Milano, Italy. Tel.: +39 02 503 15518; fax: +39 02 503 15494.
E-mail address: giovanni.muttoni1@unimi.it (G. Muttoni).

0031-0182/$ – see front matter © 2013 Elsevier B.V. All rights reserved.
http://dx.doi.org/10.1016/j.palaeo.2013.06.011

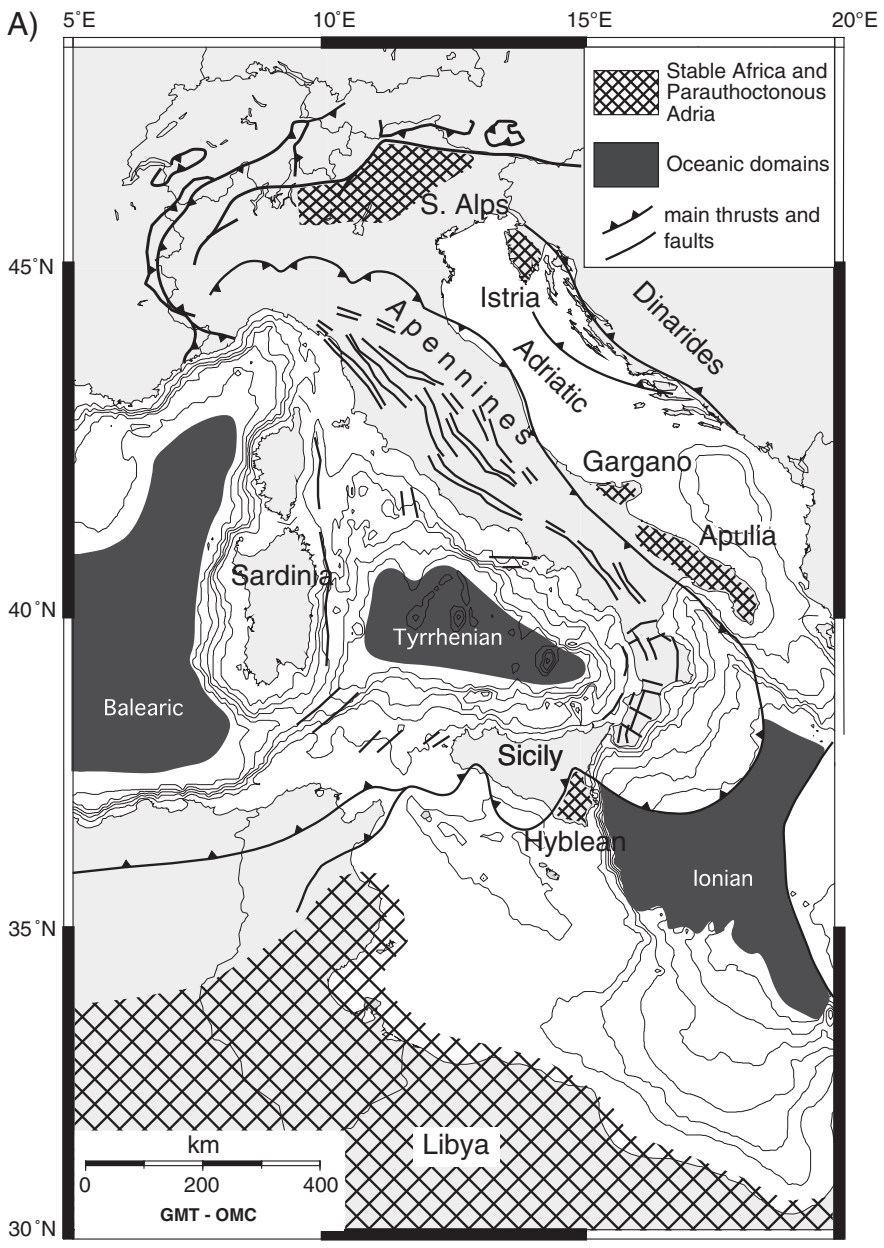
A)
5°E
10°E
15°E
20°E
45°N
40°N
35°N
30°N
Stable Africa and Parauthoctonous Adria
Oceanic domains
main thrusts and faults
S. Alps
Istria
Dinarides
Apennines
Adriatic
Gargano
Apulia
Sardinia
Tyrrhenian
Balearic
Sicily
Hyblean
Ionian
Libya
km
0
200
400
GMT - OMC

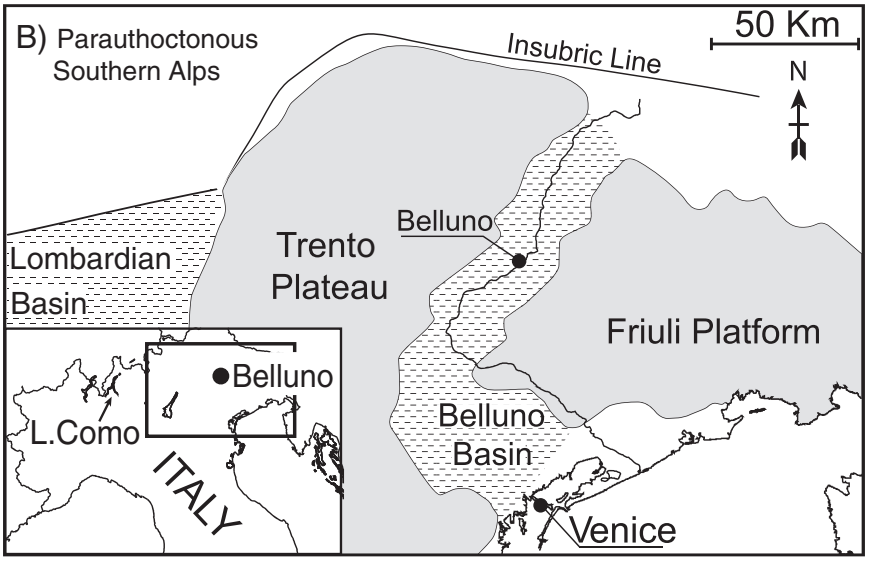
B) Parauthoctonous Southern Alps
Insubric Line
50 Km
N
Belluno
Trento Plateau
Lombardian Basin
Friuli Platform
Belluno Basin
Venice
Belluno
L.Como
ITALY

in the 1960s and 1970s came the realization that the Alps — the heart of Europe — are not European insofar as they were found to possess Early Permian paleomagnetic directions deviating from coeval directions from non-Alpine Europe by up to 50° (e.g., Van Hilten, 1962; Van Hilten and Zijderveld, 1966; Zijderveld et al., 1970). Another important outcome of these two decades of pioneering work was the realization that the Early Permian paleomagnetic directions from the Southern Alps agree reasonably well with coeval directions from Africa (Zijderveld et al., 1970), a coherence that was later proven valid also for the Mesozoic (e.g., Channell and Tarling, 1975; Channell, 1996).

Another region of Italy that received attention in the early seventies of the last century was southeastern Sicily — the undeformed Hyblean platform facing the Ionian Sea (Fig. 1A) — where different authors sampled Pliocene–Pleistocene and Upper Cretaceous basalts and concluded that no relative movement occurred between authochtonous Sicily and Africa since the Late Cretaceous (e.g., Barberi et al., 1974; Gregor et al., 1975). At broadly the same time, attention was devoted to the Umbrian Apennines of central Italy, where ample evidence for tectonic rotations was found (e.g., Lowrie and Alvarez, 1975), in apparent contrast with the findings from southeastern Sicily. However, subsequent studies on classic Mesozoic–Cenozoic sedimentary successions revealed that the Umbrian Apennines are characterized by an apparent polar wander path (APWP) that is African in shape but rotated counterclockwise by ~20–25° with respect to Africa essentially due to thrust-sheet rotations rather than lithospheric decoupling of peninsular Italy relative to Africa (Channell, 1996; Satolli et al., 2007, 2008). Somewhat similarly, Cretaceous paleomagnetic directions from the largely undeformed Adriatic foreland regions of Gargano and Istria (Fig. 1A), which were initially taken to suggest rotation of peninsular Italy relative to Africa (e.g., Heller et al., 1989), were subsequently superseded by higher quality data that indicated no such rotations (Channell, 1996).

This brief historical overview indicates that the concept of the African affinity of largely undeformed foreland regions of the Alpine–Apennine–Dinaric orogen (Istria, Gargano, Hyblean platform), as well as of parts of the deformed Southern Alps margin (see below), took shape in the 1970s (e.g., Zijderveld et al., 1970), became well established and documented since the 1990s (Van der Voo, 1993; Channell, 1996), and since then was reiterated and enhanced by inclusion of additional Permian–Triassic (Muttoni et al., 1996, 1997; Brack and Muttoni, 2000; Muttoni et al., 2001, 2003, 2010), Jurassic (Muttoni et al., 2005; Channell et al., 2010), and Paleocene–Eocene data (Dallanave et al., 2009; Agnini et al., 2011; Dallanave et al., 2012). After four decades of intensive paleomagnetic research, we conclude that Adria can be broadly divided into three regions (Fig. 1A):

1) The Apennines — the backbone of the Italian peninsula — running from Piedmont in the northwest to Sicily in the south, characterized by the ubiquitous presence of thrust sheets affected by complex vertical-axis rotations. These rotations are essentially counterclockwise in the Mesozoic–Cenozoic 'hard core' of the northern-central Apennines, from the juncture with the western Alps in Piedmont (Carrapa et al., 2003; Maffione et al., 2008) to the Emilia–Marche–Umbria Apennines (e.g., Channell et al., 1978; Hirt and Lowrie, 1988; Muttoni et al., 2001; Satolli et al., 2007, 2008), as well as in the Late Miocene Adriatic foredeep deposits at the main thrust front (Speranza et al., 1997), and essentially clockwise in the Sicilian Apennines (e.g., Channell et al., 1990). The Tyrrhenian extensional margin in the west appears largely unrotated at least since the Late Miocene (Mattei et al., 1996).
2) The substantially undeformed foreland of the Alpine–Apennine–Dinaric orogeny centered on the Adriatic Sea and exposed in Istria (Slovenia) and Gargano–Apulia (Puglia, southern Italy), as well as in southeastern Sicily (Hyblean platform) facing the Ionian Sea (Fig. 1A), which yielded Cretaceous paleomagnetic results coherent with coeval results from Africa and are therefore considered parautochthonous relative to the African craton (Channell, 1996; this study).
3) The Southern Alps represented by the Mesozoic–Cenozoic paleogeographic domains of the Trento plateau (including the Dolomites) bounded in the east by the Belluno basin and in the west by the Lombardian basin (Fig. 1B). In this segment of the Southern Alps, shortening deformation was broadly oriented N–S (e.g., Castellarin et al., 1992) and involved thick piles of Triassic platform carbonate rocks overlying Permian volcanic rocks resting above the Variscan crystalline basement, which conferred rigidity to the thrust sheets and prevented large and systematic vertical axis rotations, which are more typical of Apennine tectonics. This region of the Southern Alps, broadly spanning from Lake Como in the west to Belluno in the east (Fig. 1B), yielded Permian, Triassic, Jurassic, and Cretaceous paleomagnetic results that are *substantially* coherent with coeval data from Africa (Channell, 1996; Muttoni et al., 2003; this study), and, for this reason, they are interpreted as parautochthonous with respect to the African craton.

As several key papers have been published since the Channell (1996) review, an update of the Adria APWP for comparison with African paleomagnetic poles (hereafter paleopoles or simply poles) is warranted. In addition, it is now realized that several types of sedimentary deposits (e.g. hematite-bearing redbeds) can be affected by (sometimes large) paleomagnetic inclination flattening errors (Tauxe and Kent, 1984) that can however be detected and corrected using the elongation/inclination (E/I) statistical method of Tauxe and Kent (2004) (see also Kent and Tauxe, 2005). In this paper, we review the available paleomagnetic data of Adria from volcanic rocks or sedimentary rocks that have been corrected for inclination shallowing. We focus our analysis on sites pertaining to regions of Adria that are regarded as parautochthonous with respect to the African craton (i.e., regions #2 and #3 described above), whereas data from the Apennines (region #1), characterized by vertical axis rotations of up to ~25° (Satolli et al., 2007, 2008), are discussed but not included in our Adria compilation. Finally, we compare paleomagnetic data from parautochthonous Adria with coeval data mainly from igneous rocks from stable Africa for the construction of a composite Adria–Africa APWP.

3. Paleomagnetic poles from Adria and Africa

The paleomagnetic database of Adria and Africa adopted in this study is composed of 79 individual entries from the literature dated from the Early Permian to the Miocene (Table 1), with ages expressed relative to the Geological Time Scale 2012 of Gradstein et al. (2012). Early Permian data from the Southern Alps, and Late Cretaceous data from the Hyblean platform of southeastern Sicily, are from volcanic rocks for which no inclination shallowing is expected (Tauxe and Kent, 2004). Middle Triassic, Jurassic, Early Cretaceous, and Paleocene–Eocene data are from sedimentary rocks from the Southern Alps that we tested (and corrected) for inclination shallowing, as illustrated below.

3.1. Correction for sedimentary inclination bias

The applied method (Tauxe and Kent, 2004) consists of progressively unflattening paleomagnetic directions by decreasing the flattening parameter f (King, 1955) in the equation $\tan I_f = f \cdot \tan I_0$ (where I_f and I_0 are the measured inclination and the true inclination of the magnetic field during sedimentation, respectively) so that the directional dataset assumes an E/I pair of values that is consistent with the TK03.GAD field model (Tauxe and Kent, 2004; see also Kent and Tauxe, 2005; Tauxe et

Fig. 1. (A) Map of Adria showing the main tectonic subdivisions described in the text, including the parautochthonous regions of the Southern Alps (see panel B), Istria, Gargano–Apulia, and Hyblean platform. (B) Map of the Southern Alps with indication of parautochthonous paleogeographic units (Trento plateau, Lombardian and Belluno basins).

Table 1
Paleomagnetic data from Adria and Africa.

Entry rock unit and ref.	N	$Dec._{tc}$	$Inc._{tc}$	$a95_{tc}$	N_{45}	$Dec._{45}$	$Inc._{45}$	k_{45}	$a95_{45}$	f	Clnc	$Clnc_{(\pm)}$	Long	Lat
Early Permian (~284–276 Ma)														
Adria														
1 Southern Alps volcanics 46.0°N/11.0°E (general locality) (Muttoni et al., 2003)	7*	151.5	−25.6	8.6	–	–	–	–	–	**1.0**	–	–	236	50
2 Lugano (Ganna) Porphyries, Ticino 45.8°N/8.8°E (mean locality) (Heiniger, 1979)	4*	142.9	−20.4	10.4	–	–	–	–	–	**1.0**	–	–	242.6	42.7
3 Auccia volcanics, Lombardy 45.8°N/10.4°E (mean locality) (Heiniger, 1979)	5*	139.7	−14.1	8.2	–	–	–	–	–	**1.0**	–	–	244.9	38.1
4 Arona volcanics, Lombardy 45.7°N/8.5°E (mean locality) (Heiniger, 1979)	4*	134.9	−14.2	13.6	–	–	–	–	–	**1.0**	–	–	248.0	35.4
5 Bolzano Porphyries, Alto Adige 46.2°N/11.5°E (mean locality) (Zijderveld et al., 1970)	39*	150	−19.5	5	–	–	–	–	–	**1.0**	–	–	236[a]	45.5
6 Bolzano Porphyries, Alto Adige 46.5°N/11.3°E (mean locality) (Becke and Mauritsch, 1984)	50	155.2	−16.8	4.1	–	–	–	–	–	**1.0**	–	–	228	47
7 L.Collio & Auccia volcanics, Lombardy 45.8°N/10.2°E (mean locality) (Zijderveld and De Jong, 1969)	5*	135	−21	20	–	–	–	–	–	**1.0**	–	–	252.5	38.5
Africa														
8 Taztot Trachyandesites, Morocco 32.2°N/354°E (general locality) (Daly and Pozzi, 1976)	12″	136	−5	4.6	–	–	–	–	–	**1.0**	–	–	237	39
9 Chougrane & Mechra Volcs., Morocco 32.5°N/352.5°E (general locality) (Westphal et al., 1979)	4*	–	–	–	–	–	–	–	–	**1.0**	–	–	238	36
10 Jebel Nehoud 282 Ma, Sudan (Bachtadse et al., 2002)	8*	147.2	39.6	6.0	–	–	–	–	–	**1.0**	–	–	248[b]	46.5[b]
Australia														
11 Mt. Leyshon Intrusives Australia 20.2°S/146.3°E (Clark and Lackie, 2003)	34*	196.3	77.4	3.4	–	–	–	–	–	**1.0**	–	–	252[c]	35.5[c]
12 Tuckers Igneous Complex Australia 20.1°S/146.5°E (Clark and Lackie, 2003)	42*	188.7	75.2	3.8	–	–	–	–	–	**1.0**	–	–	249[c]	41[c]
Late Permian–Early Triassic (~260–245 Ma)														
Adria														
13 upper Bellerophon Fm. & Werfen Fm. (Siusi–Campil mbs.), Bulla section, Dolomites 46.52°N, 11.63°E (Scholger et al., 2000)	141″	335.4	15.5	3.8	138	335.5	15.0	17	3.0	**0.80**	18.5	14.8/22.6	228.9	47.5
14 upper Bellerophon Fm. & Werfen Fm. (Siusi–Campil mbs.), Siusi section, Dolomites 46.56°N, 11.57°E (Scholger et al., 2000)	181″	335.3	18.6	3.3	–	–	–	–	–	**0.8**[d]	22.8	–	230.6	49.5
15 Werfen Fm. (Siusi–Campil mbs.), Dolomites 46.5°N/11.8°E (mean locality) (Channell and Doglioni, 1994)	26*	330.8	13.0	6.6	–	–	–	–	–	**0.8**[d]	16.1	–	234.2	44.3
16 Verrucano Lombardo metasediments & redbeds combined, Lombardy 45.9°N/10.6°E (mean locality) (Kipfer and Heller, 1988)	12*	326.7	22.7	7.0	–	–	–	–	–	**0.8**[d]	37.2	–	249.1	53.0
17 Val Gardena Ss., Dolomites 46.3°N/11.8°E (mean locality) (Manzoni, 1970)	4*	328.0	13.0	18	–	–	–	–	–	**0.8**[d]	22.8	–	240.4	46.2
Africa														
18 Karoo Upper Permian redbeds, Ouberg Pass, S. Africa (32.4°S, 20.3°E) (Lanci et al., in press)	136″	308	−53	4.1	–	–	–	–	–	(1.0	–	–	272.3[b]	54.5[b])
										0.7	−62.2	−56/−73	255.0[b]	55.5[b]
										(0.6	−65.7	–	247.3[b]	55.2[b])
19 Karoo P/T boundary redbeds, Komandodrifdam, S. Africa (32.2°S, 26.1°E) (DeKock and Kirschvink, 2004)	35″	311.9	−61.6	7.6	–	–	–	–	–	(1.0	–	–	262.9[b]	58.5[b])
										0.7[e]	−69.3	–	244.2[b]	56.8[b]
										(0.6	−72.0	–	237.4[b]	55.3[b])
South America														
20 Choiyoi Volcanic Complex S America, Argentina 263 +1.6/−2.0 Ma (Domeier et al., 2011b)	35*	169.2	61.4	2.5	–	–	–	–	–	**1.0**	–	–	244.3[b]	52.4[b]
Middle–early Late Triassic (Ladinian–earliest Carnian; ~241–236 Ma)														
Adria														
21 Buchenstein Beds Belvedere, Dolomites 46.4°N/12.0°E (Brack and Muttoni, 2000)	93″	344.5	21.1	7.4	78	342.3	18.8	9	5.7	**0.81**	22.7	19.1/35.8	221.1	52.3
22 Buchenstein Beds Froetschbach, Dolomites 46.6°N/11.8°E (Muttoni et al., 1997)	92″	350.8	38.0	5.7	77	352.3	34.8	16	4.1	**0.89**	37.9	33.5/46.7	208.3	63.9
23 Val Gola Limestones Margon, Trentino 46.0°N, 11.1°E (Gialanella et al., 2001)	55″	342.5	34.0	4.7	–	–	–	–	–	**0.85**[f]	38.4	–	227.3	61.7
24 San Cassiano Fm. Stuores, Dolomites 46.6°N/11.9°E (Broglio Loriga et al., 1999)	89″	359.4	16.5	6.0	78	358.3	17.0	16	4.2	**0.57**	26.2	19.3/34.0	194.9	57.2

Africa														
25 Al-Azizia & Kaf Bates combined, Lybia 32.45°N/13.15°E (Muttoni et al., 2001)	2*/60″	–	–	–	56	347.2	5.8	33	3.3	**0.58**	10.0	5.2/15.2	219.4	60.1
Earliest Jurassic (~201 ± 1 Ma)														
Africa (Central Atlantic Magmatic Province)														
26 Draa Valley sills, Morocco (Hailwood and Mitchell, 1971)	16*	339.0	27.5	4.5	–	–	–	–	–	**1.0**	–	–	230.5 (A95 = 3.5)	65.5
27 Foum Zguid dyke, Morocco (Hailwood and Mitchell, 1971)	5*	325.0	40.0	4.0	–	–	–	–	–	**1.0**	–	–	259.0 (A95 = 4.0)	58.0
28 Foum Zguid dyke, Morocco (Silva et al., 2006)	6*	336.4	40.9	2.3	–	–	–	–	–	**1.0**	–	–	250.3 (A95 = 2.4)	67.8
29 Foum Zguid dyke, Morocco (Palencia-Ortas et al., 2011)	12*	336.8	39.3	3.9	–	–	–	–	–	**1.0**	–	–	247.9 (A95 = 3.9)	67.9
30 Ighrem dyke, Morocco (Palencia-Ortas et al., 2011)	11*	348.4	42.1	6.8	–	–	–	–	–	**1.0**	–	–	238.2 (A95 = 6.7)	78.4
31 CAMP lavas, Morocco (Font et al., 2011)	99″	333.5	27.0	3.0	–	–	–	–	–	**1.0**	–	–	241.6 (A95 = 2.6)	60.0
32 Liberian dikes and sills, NW Africa (Dalrymple et al., 1975)	25*	–	–	–	–	–	–	–	–	**1.0**	–	–	242.4 (A95 = 5.3)	68.5
33 Hank volc., North Mauritania (Sichler et al., 1980)	13*	342	24	4.1	–	–	–	–	–	**1.0**	–	–	232.0 (A95 = 4.1)	69.4
34 Hodh volc., South Mauritania (Sichler et al., 1980)	13*	342.5	18.5	6.1	–	–	–	–	–	**1.0**	–	–	240.2 (A95 = 6.1)	71.4
35 Freetown Complex, Sierra Leone (Hargraves et al., 1999)	13*	174.8	−6.9	6.2	–	–	–	–	–	**1.0**	–	–	212.7 (A95 = 5.6)	82.9
Early Jurassic (Sinemurian; ~199–191 Ma)														
Adria														
36 Colle di Sogno, Lombardy (Channell et al., 2010)	85″	335.3	54.6	2.3	85	–	–	–	–	**1.0**	–	–	258.3 (A95 = 2.7)	68.5
Early Jurassic (Toarcian) (~183 ± 1 Ma)														
Karoo Igneous Province, South Africa														
37 Stromberg lavas, Lesotho (Van Zijl et al., 1962)	74*	–	–	–	–	–	–	–	–	**1.0**	–	–	262.9[b] (A95 = 15)	78.6[b]
38 Lesotho lavas (Kosterov and Perrin, 1996)	28*	–	–	–	–	–	–	–	–	**1.0**	–	–	270.3[b] (A95 = 3.7)	79.3[b]
39 Karoo mean pole South Africa, various localities (Hargraves et al., 1997)	84*/6**	–	–	–	–	–	–	–	–	**1.0**	–	–	278.1[b] (A95 = 3.3)	76.9[b]
40 Naude's Nek lavas, South Africa (Moulin et al., 2011)	19*	342.8	−54.0	4.7	–	–	–	–	–	**1.0**	–	–	275.2[b] (A95 = 5.8)	82.9[b]
Late Jurassic (Callovian–Oxfordian; ~164–157 Ma)														
Adria														
41 Colle Sogno (CS), Lombardy (45.7°N, 9.5°E) sites CS8 + CS9 combined (Red Cherts-base Rosso Aptici) Callovian–Oxfordian (Muttoni et al., 2005)	19″	350.9	18.0	4.9	19	–	–	–	–	–	–	–	204.4	52.6
42 Torre de' Busi (TB), Lombardy (45.7°N, 9.5°E) Meter levels 48–54 (Red Cherts-base Rosso Aptici) Callovian–Oxfordian (Channell et al., 2010)	25″	331.2	21.7	3.8	25	–	–	–	–	–	–	–	234.0	47.7
43 Passo del Branchetto (PB), Veneto 45.6°N/11°E Fonzaso Cherty Limestone Late Oxfordian (Channell et al., 2010)	54″	299.3	28.1	3.5	54	–	–	–	–	**0.72**	36.6	29.0/48.0	275.1	34.7
Late Jurassic (Early Tithonian, Chron 22; ~151 ± 1 Ma)														
Adria														
44 Colme di Vignola, Trentino 45.8°N, 10.9°E (Channell et al., 2010)	87″	304.5	28.5	2.5	87	–	–	–	–	**1.0**	–	–	266.2	34.7
45 Foza, Veneto 45.9°N, 11.6°E (Channell et al., 2010)	41″	308.2	30.7	1.9	41	–	–	–	–	**1.0**	–	–	264.7	38.1
46 Frisoni, Veneto 45.9°N, 11.7°E (Channell et al., 2010)	47″	309.2	33.2	2.1	47	–	–	–	–	**1.0**	–	–	265.4	39.9

(continued on next page)

Table 1 (*continued*)

Entry rock unit and ref.	N	$Dec._{tc}$	$Inc._{tc}$	$a95_{tc}$	N_{45}	$Dec._{45}$	$Inc._{45}$	k_{45}	$a95_{45}$	f	Clnc	$Clnc_{(\pm)}$	Long	Lat
Late Jurassic (Mid–Late Tithonian, Chrons 20–21; ~147 ± 1.5 Ma)														
Adria														
47 Torre de' Busi, Lombardy 45.7°N, 9.5°E Chrons 20 & 21n combined (Channell et al., 2010)	312″	312.4	30.9	1.6	309	312.3	30.9	30	1.5	**0.76**	38.3	32.5/43.9	263.9	44.4
48 Foza, Veneto 45.9°N, 11.6°E Chrons 20 & 21 (Channell et al., 2010)	73″	312.9	33.2	2.1	73	–	–	–	–	**0.98**	33.6	32.6/45.8	262.2	42.5
49 Frisoni, Veneto 45.9°N, 11.7°E Chrons 20 & 21 (Channell et al., 2010)	122″	316.9	30.0	1.7	122	–	–	–	–	**0.81**	35.3	30.2/44.8	259.6	45.9
Early Cretaceous (Berriasian, Chrons 17–19; ~143 ± 2 Ma)														
Adria														
50 Colme di Vignola, Trentino 45.8°N, 10.9°E Chrons 17–19 (Channell et al., 2010)	58″	309.0	34.8	2.8	58	–	–	–	–	**0.90**	37.8	34.3/47.8	267.8	41.9
51 Foza, Veneto 45.9°N, 11.6°E Chrons 17–19 (Channell et al., 2010)	135″	314.1	36.3	1.1	135	–	–	–	–	**0.86**	40.6	36.5/47.5	265.9	46.7
52 Frisoni, Veneto 45.9°N, 11.7°E Chrons 18–19 (Channell et al., 2010)	113″	319.4	35.0	1.4	113	–	–	–	–	**0.81**	40.8	35.3/47.8	261.1	50.3
Africa														
53 Swartruggens kimberlite and Bumbeni syenite complex (~145 Ma) southern Africa (Hargraves et al., 1997)	6*	–	–	–	–	–	–	–	–	**1.0**	–	–	283.8[b] (A95 = 6.3)	39.3[b]
North America														
54 Ithaca kimberlite (~143 Ma) North America (Van Fossen and Kent, 1993)	7*	317.3	58.9	2.6	–	–	–	–	–	**1.0**	–	–	266.4[c] (A95 = 3.8)	35.6[c]
Early Cretaceous (Hauterivian–Barremian; ~134–126 Ma)														
55 Northern Italy Maiolica Capriolo, Lombardy 45.6°N, 10.0°E (Channell et al., 1987)	252″	331.7	41.0	3.8	215	334.7	36.1	16.2	2.5	**0.78**	43.6	37.4/50.0	244.6	61.8
56 Cismon, Veneto 46.0°N, 11.8°E (Channell et al., 2000)	239″	317.4	30.4	2.4	230	315.8	29.2	32.2	1.7	**0.56**	45.1	38.7/51.3	268.3	50.2
57 Polaveno, Lombardy 45.7°N, 10.1°E (Channell and Erba, 1992)	504″	319.3	37.3	1.4	494	319.0	36.6	27.7	1.2	**0.82**	42.1	38.3/45.8	262.2	51.2
58 San Giovanni, Lombardy 45.7°N, 10.1°E (Channell and Erba, 1992)	86″	323.4	36.0	2.7	85	323.3	35.5	39.4	2.5	**0.94**	37.1	34.6/45.5	253.2	51.4
59 Val del Mis, Veneto 46.2°N, 12.1°E (Channell et al., 1993)	158″	308.8	28.9	3.1	153	308.8	28.9	18.2	2.7	**0.86**	32.7	28.4/39.5	266.2	40.0
Africa														
60 Etendeka, Kaoko lavas, Namibia (Gidskehaug et al., 1975)	40*	315.0	−44.5	3.1	–	–	–	–	–	**1.0**	–	–	263.5[b] (A95 = 3.1)	55.9[b]
61 Etendeka, Messum gabbros, Namibia (Renne et al., 2002)	6*	323.7	−48.7	3.4	–	–	–	–	–	**1.0**	–	–	260.8[b] (A95 = 4.5)	57.7[b]
Late Cretaceous (Cenomanian–Campanian; ~100–71 Ma)														
Adria														
62 Iblei volcanics (~84–71 Ma) Capo Passero, Sicily 36.7°N, 15.1°E (Grasso et al., 1983)	12*	173.6	−31.2	7.4	–	–	–	–	–	**1.0**	–	–	212.3	69.3
63 Iblei volcanics (~84–71 Ma) Capo Passero, Sicily 36.7°N, 15.1°E (Gregor et al., 1975)	15*	162.9	−30.1	9.8	–	–	–	–	–	**1.0**	–	–	236	64
64 Iblei volcanics (~84–71 Ma) Capo Passero, Sicily 36.7°N, 15.1°E (Barberi et al., 1974)	8*	165	−26	7.0	–	–	–	–	–	**1.0**	–	–	229	63
65 Iblei volcanics (~84–71 Ma) Capo Passero, Sicily 36.7°N, 15.1°E (Schult, 1973)	19*	167	−22	7.1	–	–	–	–	–	**1.0**	–	–	223.3	62.1
Africa														
66 Group 1 Kimberlites (~100–81 Ma) South Africa, 29°S, 24°E (Hargraves, 1989)	14*	–	–	–	–	–	–	–	–	**1.0**	–	–	226.1 (A95 = 5.2)	64.1
67 Madagascar volcanics (87 ± 3 Ma) (Torsvik et al., 1998)	8**	–	–	–	–	–	–	–	–	**1.0**	–	–	230.3 (A95 = 5.5)	68.5

Paleocene–Eocene (~65–36 Ma)															
Adria															
68 South Ardo, Veneto 46.0°N, 12.1°E (Dallanave et al., 2012)	239″	356.5	34.8	2.1	233	356.4	34.4	25.1	1.9	**0.60**	48.7	42.6/54.2	203.5	73.7	
69 Cicogna, Veneto 46.1°N, 12.2°E (Dallanave et al., 2009)	229″	356.2	27.6	2.9	220	355.7	27.3	15.2	2.5	**0.41**	51.1	41.9/58.4	207.0	75.0	
70 Alano di Piave, Veneto 45.9°N, 11.9°E (Agnini et al., 2011)	104″	350.8	40.5	4.5	95	351.5	37.2	18.7	3.4	**0.62**	50.8	40.2/62.4	220.0	74.5	
Africa															
71 Wadi Abu Tereifiya volcanics, Egypt (Hussain et al., 1979)	12*	007.9	20.8	5.8	–	–	–	–	–	**1.0**	–	–	189.4	69.4	(A95 = 4.6)
72 Africa plate (DSDP524, ODP707, Gubbio), inclination-only data, Paleocene (Schneider and Kent, 1990)	3*	–	–	–	–	–	–	–	–	0%G3	–	–	213	70.1	
Oligocene (34–23 Ma)															
Africa															
73 Yemen Traps (~30 Ma) (Riisager et al., 2005)	48*	–	–	–	–	–	–	–	–	**1.0**	–	–	224.4[g]	77.8[g]	(A95 = 3.6)
74 Ethiopian Traps (~30 Ma) (Kidane et al., 2002)	76*	–	–	–	–	–	–	–	–	**1.0**	–	–	209.4	78.7	(A95 = 3.4)
75 Africa plate (DSDP523, ODP706, Gubbio), inclination-only data, Oligocene (Schneider and Kent, 1990)	3*	–	–	–	–	–	–	–	–	5%G3	–	–	193	75.9	
Miocene (23–5 Ma)															
Africa															
76 Jebel Soda alkali basalts, Libya (16–8 Ma according to Bardintzeff et al., 2012) (Schult and Soffel, 1973)	12*	359.9	31.6	8.3	–	–	–	–	–	**1.0**	–	–	196.1	79.4	(A95 = 7.4)
77 Turkana volcanics (~17 Ma) (Reilly et al., 1976)	62*	004.1	01.7	3.1	–	–	–	–	–	**1.0**	–	–	163.3	84.6	(A95 = 2.3)
78 Canaries–Madeira volcanics (Miocene) (Watkins, 1973)	99*	–	–	–	–	–	–	–	–	**1.0**	–	–	114.4	81.9	(A95 = 3.5)
79 Fuerteventura volcanics (Storetvedt et al., 1979)	10*	004.3	31.0	5.2	–	–	–	–	–	**1.0**	–	–	146.2	77.8	(A95 = 5.2)

Notes: Entry = reference entry number of paleomagnetic data from magmatic (bold) and sedimentary (regular font) units; N = number of samples/sites/areas (* = number of sampling sites; ** = number of sampling areas [each with multiple sites]; ″ = number of samples); Dec.tc = mean declination in tilt corrected coordinates (expressed in °E); $Inc._{tc}$ = mean declination in tilt corrected coordinates (expressed in °); $a95_{tc}$ = half cone of confidence at 95% level around the mean in tilt corrected coordinates (expressed in °); N_{45} = number of paleomagnetic directions with VGP > 45° and VGP < −45°; $Dec._{45}$ = mean declination of samples with VGP > 45° and VGP < −45° (expressed in °E); $Inc._{45}$ = mean inclination of samples with VGP > 45° and VGP < −45° (expressed in °); k_{45} = Fisher precision parameter of mean direction of samples with VGP > 45° and VGP < −45°; $a95_{45}$ = half cone of confidence at 95% level around the mean direction of samples with VGP > 45° and VGP < −45° (expressed in °); f = flattening factor; Clnc = E/I corrected mean inclination (expressed in °); $Clnc_{(\pm)}$ = error of Clnc (expressed in °); Long = Longitude of paleomagnetic pole (expressed in °E); Lat = Latitude of paleomagnetic pole (expressed in °N); A95 = half cone of confidence at 95% level around the paleomagnetic pole (expressed in °).

[a] Erroneously reported as 239°E in Van der Voo (1993) and Muttoni et al. (2003).

[b] Rotated to northwest Africa (=Adria) coordinates using rotation parameters of Lottes and Rowley (1990).

[c] Rotated to NW Africa using rotation parameters of Klitgord and Schouten (1986).

[d] f value assumed (same of entry #13).

[e] f value assumed (same of entry #18).

[f] f value assumed (= mean of f values from entries #21 and #22 from Buchenstein Beds).

[g] Rotated to northwest Africa (=Adria) coordinates using rotation parameters of Besse and Courtillot (2002).

al., 2008; Tauxe, 2010). To evaluate the robustness of this estimate, the analyses have been repeated by generating 5000 bootstrapped datasets for each site using L. Tauxe's PmagPy software package.

One of the characteristics of the TK03.GAD model is that it implies circularly symmetric virtual geomagnetic pole (VGP) distributions at all latitudes (Tauxe and Kent, 2004). We therefore evaluated the degree of circular symmetry of the VGPs before and after E/I correction through quantile–quantile (Q–Q) plots (see Tauxe, 2010 for details). In a Q–Q plot, the declination values of a VGP distribution are considered compatible with a reference (circularly symmetric) distribution of values (in our case, from the TK03.GAD model) if they plot along a straight line. We analyzed a total of 20 individual VGP distributions from sedimentary rocks from Adria included in our database (Table 1), finding that in almost all cases, they tend to align along a straighter line, hence becoming more uniformly distributed around the mean, after application of the E/I test. This analysis is illustrated in the representative case studies from Stuores (Middle–Late Triassic), Passo del Branchetto (Late Jurassic), Cismon (Early Cretaceous), and South Ardo (Paleocene–Eocene) of Supplementary Fig. 1 plotted before (panel A) and after (panel B) application of the E/I test. In general, 15 (out of a total of 20) VGP distributions analyzed were non-circularly distributed before the application of the E/I test; 7 of these non-circular distributions became circularly distributed at the 95% level of confidence after application of the E/I test (Tauxe, 2010), whereas in most of the remainder cases, the degree of circularity increased, albeit only moderately.

The f values obtained by the E/I test were applied to correct the mean paleomagnetic directions and poles of the sedimentary rocks in our compilation (Table 1). For some Late Permian–Early Triassic results, the f values could not be determined experimentally, and had to be estimated by other means (see below). Where possible, data from volcanic rocks from Africa have been used for comparison with corrected data from Adria to construct a composite, inclination flattening-free, Adria–Africa APW path for comparison with paths from the literature (Besse and Courtillot, 2002; Torsvik et al., 2008; Kent and Irving, 2010; Torsvik et al., 2012).

3.2. Early Permian

Among the several paleomagnetic poles from Early Permian volcanic rocks of the Southern Alps published since the pioneering work of Van Hilten (1960), we selected seven entries with adequate number of fully demagnetized samples from localities distributed in longitude across almost the entire Southern Alps (Table 1, entries #1–7). These poles can be confidently attributed to the same period of volcanism dated by means of U/Pb to ~284–276 Ma (Muttoni et al., 2003; Schaltegger and Brack, 2007) and are defined by characteristic magnetizations of reverse polarity most likely acquired during the Permo-Carboniferous Reversed (PCR) "Kiaman" Superchron. These paleopoles are relatively well grouped (Fig. 2A, black dots) around a mean at Long = 241.7°E, Lat = 42.7°N (Fig. 2A, small black star) albeit with an overall distribution that is slightly elongated probably due to small (but non-systematic) relative rotations of widely separated sites.

Two entries, based on sparse data from presumably coeval igneous rocks from Morocco (Table 1, entries #8–9), yield similar pole positions (Fig. 2A, gray stars). More insightful for a test of Adria–Africa coherence, however, is the more recent and statistically robust pole from the Jebel Nehoud ring complex of Sudan, dated at 280 ± 2 Ma with K/Ar on single crystals of biotite and horneblende (Bachtadse et al., 2002; Table 1, entry #10) that also falls very close to the Southern Alps paleopoles of similar age (Fig. 2A, gray hexagon). The seven paleopoles from the Southern Alps and the three paleopoles from Africa (Morocco and Sudan) are used to compute a mean paleopole for Adria–Africa located at Long = 241.6°E, Lat = 42.0°N (A_{95} = 4.4°; Table 2) that is entirely based on data from volcanic rocks and is therefore considered free from inclination shallowing. This mean paleopole, when compared to the coeval data from Europe, again from volcanic rocks, supports the Irving (1977) Pangea B model (Muttoni et al., 2003; but see Domeier et al., 2011a, versus Aubele et al., 2012, for an update on the Pangea B controversy). Notably, two additional paleopoles from the Mount Leyshon and Tuckers intrusions of Australia dated at 286 ± 2 Ma (Clark and Lackie, 2003; Table 1, entries #11 and #12), when rotated into northwest African (=Adria) coordinates using the rotation parameters of Lottes and Rowley (1990), also fall very close to the Adria–African poles (Fig. 2A, gray triangles), and support Pangea B in the Early Permian (Clark and Lackie, 2003).

3.3. Late Permian–Early Triassic

Five Late Permian–Early Triassic paleopoles used in our compilation (Table 1, entries #13–17) come from the Southern Alps. Two of them come from the Bulla and Siusi sections from the Dolomites, which have been studied for magnetostratigraphy, from the Upper Permian Bellerophon Formation to the Lower Triassic Werfen Formation (Scholger et al., 2000). We obtained a digital listing of the characteristic component directions of the Bulla section (Scholger, pers. comm.), and ran a standard E/I test (Supplementary Fig. 2A), obtaining a flattening factor f = 0.80. This was applied to the mean paleomagnetic inclination to yield a flattening-free paleomagnetic pole (Table 1, entry #13). For the coeval Siusi section (Table 1, entry #14), as well as for the remainder of the entries used in our compilation, namely the Lower Triassic Siusi and Campil members of the Werfen Formation from the Dolomites (#15; Channell and Doglioni, 1994), the Upper Permian Verrucano Lombardo metasedimentary rocks and redbeds combined from Lombardy (#16; Kipfer and Heller, 1988), and the Upper Permian Val Gardena Sandstones from the Dolomites (#17; Manzoni, 1970), we could not run an E/I test due to insufficient numbers of independent samples at each sampled site, and we therefore applied the same flattening factor obtained at Bulla (f = 0.8), assuming a similar response of these broadly similar rock types to sedimentary inclination flattening processes.

The Late Permian–Early Triassic paleopoles from the Southern Alps (Fig. 2B) are compared to the paleopole of Lanci et al. (in press) from South Africa obtained by averaging N = 136 normal and reverse polarity characteristic magnetizations from Upper Permian redbeds of the lower Beaufort Group at Ouberg Pass, Karoo basin, that are regarded as primary in age and only partially overprinted by the emplacement of the Jurassic Karoo Large Igneous Province (LIP) (Lanci et al., in press). These characteristic magnetizations have been corrected for sedimentary inclination shallowing obtaining a flattening factor f = 0.7 (Lanci et al., in press; Table 1, entry #18). We note that before unflattening, the Ouberg Pass paleopole, rotated to northwest Africa coordinates using rotation parameters of Lottes and Rowley (1990), falls far to the east of the Adria paleopoles, yet with progressive unflattening, the paleopole moves towards the Adria paleopoles such that for f = 0.7, the original paleopole discrepancy is substantially reduced (and by assuming that f = 0.6, it would be virtually eliminated) (Fig. 2B). Similarly, the South African paleopole from Permian–Triassic boundary redbeds at Komandodrifdam, Karoo basin, considered to carry primary magnetizations and to be substantially free from later remagnetization events (DeKock and Kirschvink, 2004; Table 1, entry #19), moves towards Adria paleopoles for flattening factors progressively decreasing from 1.0 (no flattening) to 0.6 (Fig. 2B). As no E/I test is available for the sparse (N = 35) data from Komandodrifdam, we adopted a value of f = 0.7 as derived from Ouberg Pass.

The Late Permian–Early Triassic overall mean paleomagnetic pole of Adria–Africa is based on five entries from Adria, corrected for inclination shallowing assuming a flattening factor of 0.8 as deduced from Bulla, and two entries from the Karoo basin, assuming a flattening factor of 0.7 as deduced from Ouberg Pass. This overall mean paleopole (Table 2) differs by 4°–7° from previous Late Permian–Early Triassic

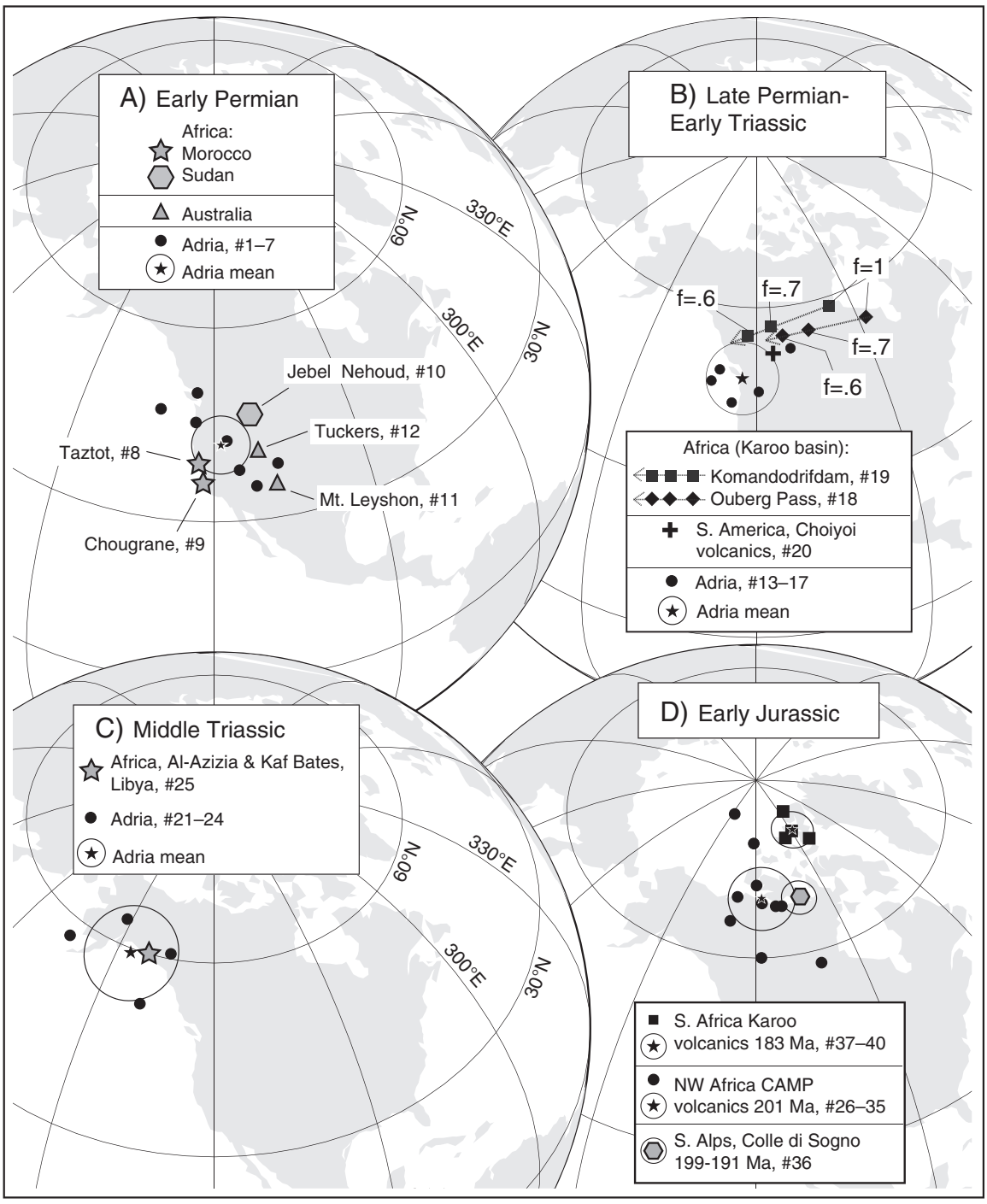

Fig. 2. Paleomagnetic poles corrected for inclination shallowing from paraautochthonous Adria for the Early Permian (A), Late Permian–Early Triassic (B), Middle Triassic (C), and Early Jurassic (D) compared with coeval poles mainly from Africa; see Table 1 for paleopole entries (#) and text for discussion.

mean paleopoles based on data from the Southern Alps without E/I correction (Muttoni et al., 1996, 2009; Angiolini et al., 2013).

There are no data from Upper Permian volcanic rocks from Africa that can be used to check the validity of our assumptions regarding flattening corrections in the Verrucano–Valgardena (or Karoo) sedimentary rocks. Notably, the only well-dated entry from volcanic rocks of comparable age from outside Adria–Africa (not included in our Adria–Africa APWP) comes from the Choiyoi Volcanic Complex of Argentina, South America, dated at about 263 (+1.6/−2.0) Ma (Table 1, entry #20; Domeier et al., 2011b), which, when rotated to northwest Africa (=Adria) coordinates using rotation parameters of Lottes and Rowley (1990), falls at Long = 244.3°E, Lat = 52.4°N, very close to the overall mean paleomagnetic pole of Adria–Africa (Fig. 2B).

3.4. Middle Triassic

Several magnetostratigraphic investigations on biostratigraphically dated Tethyan limestones with radioisotopically dated tuff intervals of Middle Triassic age from the Dolomites have been conducted since the late 1990s (see Hounslow and Muttoni, 2010, for a review). We accepted in our compilation (Table 1) the paleomagnetic data from the Belvedere section (Brack and Muttoni, 2000; entry #21), the Frötschbach section (Muttoni et al., 1997; entry #22), the Margon–Val Gola section (Brack

Table 2
The Adria–Africa apparent polar wander path.

Entry	Unit	CA	WA	RA	Long	Lat	A95	N	K
76–79	Africa	14	23–5	Miocene	156.1	82.1	6.8	4	185
73–75	Africa	28	34–23	Oligocene	208.1	77.8	5.7	3	470
68–72	Adria/Africa	50	65–36	Paleocene–Eocene	205.9	72.8	4.1	5	342
62–67	Adria/Africa	85	100–71	Cenomanian–Campanian	226.5	65.3	3.6	6	340
55–61	Adria/Africa	130	134–126	Hauterivian–Barremian	260.6	52.8	6.3	7	93
47–52	Adria	145	147–143	Mid Tithonian–Berriasian	263.5	45.3	3.1	6	463
44–46	Adria	151	152–150	Early Tithonian	265.4	37.6	4.1	3	895.5
Jurassic 'monster pole shift'									
37–40	Africa	183	184–182	Toarcian	271.5	79.5	3.2	4	821.5
26–36	Africa/Adria	201	202–200	Earliest Jurassic	243.8	69.3	4.6	11	98
21–25	Adria/Africa	238	241–236	Ladinian–Early Carnian	214.2	59.6	7.6	5	104
13–19	Adria/Africa	252	260–245	L. Permian–E. Triassic	239.7	50.7	5.8	7	109
1–10	Adria/Africa	280	284–276	E. Permian	241.6	42.0	4.4	10	120.5

Notes: Entry = reference entry number of paleomagnetic data listed in Table 1 and text; CA = Central Age window, in Ma; WA = Age window, in Ma; RA = relative age window; Long, Lat = longitude and latitude of mean paleopole; A95 = radius of 95% confidence circle around the mean paleopole; N = number of paleopoles; K = Fisher precision parameter.

et al., 2001; Gialanella et al., 2001; entry #23), and the Stuores section (Broglio Loriga et al., 1999; entry #24). Data from Belvedere, Frötschbach, and Margon–Val Gola come from the Middle Triassic Buchenstein Beds that include Pietra Verde ash layers, of which two are from the Lower and Upper Pietra Verde, respectively, and have been dated using U/Pb on single zircon crystals to 241.2 (+0.8, −0.6) Ma and 238.0 (+0.4, −0.7) Ma (Brack et al., 1996; Mundil et al., 1996), indicating an average sediment accumulation rate for the Buchenstein Beds of ~10 m/m.y. (Brack and Muttoni, 2000; Muttoni et al., 2004). The Lower Pietra Verde ash layer at 241.2 Ma is closely tied to the Anisian–Ladinian boundary based on ammonoids (Brack et al., 2005), whereas the Upper Pietra Verde ash layer at 238.0 Ma falls within the Ladinian *Archelaus* ammonoid zone (Muttoni et al., 2004; Brack et al., 2005). We obtained flattening factors f = 0.81 and 0.89 for Belvedere and Frötschbach rocks, respectively (Supplementary Fig. 2B, C; Table 1), whereas for Margon–Val Gola, we could not access the original data to run an E/I test, and we therefore assumed an average flattening factor of 0.85 derived from Belvedere and Frötschbach rocks (Table 1).

The 160 m-thick Stuores section of the San Cassiano Formation is the current global boundary stratotype section and point (GSSP) for the base of the Carnian (Broglio Loriga et al., 1999; Mietto et al., 2012). The section itself does not contain numerical age constraints, but an estimated age of ~237 Ma for the Ladinian–Carnian boundary has been recently proposed from new U/Pb zircon age data from the stratotype area (Mietto et al., 2012; see also Gradstein et al., 2012). For Stuores rocks, we obtained a flattening factor of 0.57 (Supplementary Fig. 2D; Table 1), which is among the lowest values recorded in our database, although we regard it as compatible with the lithology of the section, rich in (compressible) marls alternating with volcanoclastic and carbonate turbidites (Broglio Loriga et al., 1999). In our compilation, we exclude data from the ~110 m-long Seceda drill-core from the Dolomites that spans a complete sequence of Middle Triassic Buchenstein Beds (Muttoni et al., 2004), as this core was only approximately oriented with respect to geographic north using bedding attitude. In addition, we did not consider data from the Pedraces section (Brack and Muttoni, 2000) which are too sparse, as well as the (also sparse) data from the Ladinian–Carnian volcanic rocks of Manzoni (1970), as samples were retrieved from sites of uncertain stratigraphy and were subjected to only alternating field (AF) demagnetization.

The corrected paleomagnetic poles from Belvedere, Frötschbach, Margon–Val Gola, and Stuores (Fig. 2C) of Ladinian–Early Carnian age (~241–235 Ma) are compared with the only dataset from Africa of comparable age from the Al-Azizia and Kaf Bates sections of Libya (Muttoni et al., 2001; Table 1, entry #25), that we combined in order to perform a more robust E/I test, obtaining a flattening factor of 0.58 (Supplementary Fig. 2E; Table 1). The corrected paleomagnetic pole from these two African sections is compatible with the paleomagnetic poles from the Dolomites, falling within the confidence interval of their mean paleopole (Fig. 2C). This allows us to calculate an overall mean paleomagnetic pole for Adria–Africa based on four entries from the Dolomites and one from Libya (Table 2).

3.5. Early Jurassic

Our Early Jurassic database (Table 1, #26–40) includes one entry from Adria: the Sinemurian (~199–191 Ma) marine limestones from the Colle di Sogno section from Lombardy (Channell et al., 2010), which we found to be free from inclination flattening (f = 1) (Table 1; entry #36). Data from Rhaetian–Lower Hettangian sedimentary rocks from Lombardy (Muttoni et al., 2010) were not considered because the resolved magnetizations do not pass a reversal test, probably due to the presence of an unresolved magnetization overprint (Muttoni et al., 2010). Most data for the Early Jurassic come from the ~201 Ma Central Atlantic Magmatic Province (CAMP) and the ~183 Ma Karoo Large Igneous Province (LIP) from Africa, both of which are regarded as free from inclination flattening (Table 1).

For the Africa CAMP extrusions, we used data from the Draa Valley sills of Morocco (Hailwood and Mitchell, 1971; entry #26), the Foum Zguid and Ighrem dykes of Morocco (Hailwood and Mitchell, 1971; Silva et al., 2006; Palencia-Ortas et al., 2011; entries #27–30), the CAMP lavas of Morocco (Font et al., 2011; #31), the Liberian dikes and sills of northwest Africa (Dalrymple et al., 1975; #32), the Hank and Hodh volcanic rocks from Mauritania (Sichler et al., 1980; #33–34), and the Freetown Complex of Sierra Leone (Hargraves et al., 1999; #35). We follow Kent and Irving (2010) in considering these entries as all likely to belong to the CAMP event, which was presumably emplaced over a short (1–2 Myr) interval at around 201 Ma (Kent and Irving, 2010, and references therein). For the Toarcian Karoo LIP, presumably emplaced over a short (1–2 Myr) interval at around 183 Ma (Courtillot and Renne, 2003; but see Jourdan et al., 2005 who proposed a longer duration of emplacement), we used data from the Stromberg and Lesotho lavas of Lesotho (Van Zijl et al., 1962; Kosterov and Perrin, 1996; #37–38), the Karoo mean pole from several extrusions in South Africa (Hargraves et al., 1997; #39), and the Naude's Nek lavas of South Africa (Moulin et al., 2011; #40). These entries from South Africa have been rotated to northwest Africa (=Adria) coordinates using rotation parameters of Lottes and Rowley (1990) (Fig. 2D).

The CAMP and Karoo paleomagnetic poles are compared with the Sinemurian (~199–191 Ma) Colle di Sogno (Adria) paleopole (Fig. 2D). The Colle di Sogno paleopole falls relatively close to the immediately older CAMP paleopoles, whereas the younger Karoo paleopoles lie at higher northern latitudes. We therefore averaged entries from the CAMP and Colle di Sogno to calculate an overall mean paleopole for Africa–Adria, to which we attach a mean age of ~201 Ma because the pole is essentially based on ~201 Ma CAMP data (Table 2). Paleopole entries from the Karoo LIP define an overall mean paleomagnetic pole

valid for Africa at ~183 Ma, which lies north of the CAMP mean paleopole (Fig. 2D; Table 2).

3.6. Middle–Late Jurassic

Middle Jurassic data from Adria are sparser than those of Late Jurassic age. Hence, we opted to start from the Late Jurassic before attempting to fill in the Middle Jurassic gap. Late Jurassic data from Adria come from magneto-biostratigraphically dated sections from the Trento plateau and the Lombardian basin in the Southern Alps (Channell et al., 2010). These sections have been successfully correlated to marine magnetic anomalies (M sequence) and used to improve the definition of the Jurassic magnetic polarity time scale (Channell et al., 2010). A total of nine entries have been checked and corrected for inclination shallowing (Table 1; entries #44–52). Three entries (#44–46) from Colme di Vignola, Foza, and Frisoni sections, dated to polarity chron CM22 at ~151 ± 1 Ma in the Early Tithonian, show no evidence of inclination shallowing (f = 1). Three entries (#47–49) from Torre de' Busi, Foza, and Frisoni sections, dated to polarity chrons CM20–21 at ~147 ± 1.5 Ma in the Mid–Late Tithonian, yield flattening factors ranging between 0.98 and 0.76 (Supplementary Fig. 3A–C), whereas three other entries (#50–52) from Colme di Vignola, Foza, and Frisoni, dated to Berriasian polarity chrons CM17–19 at ~143 ± 2 Ma, yield flattening factors between 0.90 and 0.81 (Supplementary Fig. 3E–F). The three Early Tithonian (~151 Ma) corrected paleopoles fall close to each other and to the south of the three Mid–Late Tithonian (~147 Ma) and the three Berriasian (~143 Ma) corrected paleopoles, which are also located close to each other (Fig. 3). We therefore calculated an overall mean paleomagnetic poles for Adria at 151 ± 1 Ma in the Early Tithonian, and an overall mean paleopole again for Adria at 147–143 Ma (mean of 145 ± 2 Ma) in the Mid Tithonian–Berriasian (Table 2).

There are few Middle–Late Jurassic data from igneous rocks from Africa that can be used for comparison with data from Adria. A paleomagnetic pole combining data from the Swartruggens kimberlite and the Bumbeni syenite complex of southern Africa, dated to about 145 Ma (Hargraves et al., 1997) and rotated to northwest Africa (=Adria) coordinates using rotation parameters of Lottes and Rowley (1990) (Table 1, entry #53), falls somewhat to the east of (albeit encouragingly not too far from) the presumably coeval paleopoles from Adria (Fig. 3). The Ithaca kimberlite paleopole (~143 Ma) from North America of Van Fossen and Kent (1993), rotated to northwest Africa coordinates using rotation parameters of Klitgord and Schouten (1986), is similar in location (Fig. 3). The poorly dated Swartruggens–Bumbeni paleopole and the North American Ithaca paleopole have, however, not been used to calculate the Late Jurassic part of the Adria–Africa APWP. This segment is entirely based on data from Adria (Table 2).

The ~151 Ma mean paleopole from Adria is displaced to the south by ~40° on a great circle relative to the ~183 Ma Karoo LIP mean paleopole from Africa (Fig. 3) and the Sinemurian (~199–191 Ma) paleopole from Colle di Sogno, Adria (Fig. 2D). A polar shift of similar magnitude and age has also been observed in data from North America and other cratons, and was referred to as the Jurassic 'monster shift' (Kent and Irving, 2010; see also Section 4). No reliable paleopoles are available from both the global APWP of Kent and Irving (2010) and our Adria–Africa APWP to describe the details of this Jurassic 'monster shift'. Only three paleomagnetic sites with a relatively limited total number of samples are available for Adria from the time interval of main pole shift comprised between the ~183 Ma Karoo LIP paleopole and the ~151 Ma Adria paleopole: these sites define (i) a paleopole based on N = 19 characteristic magnetizations from Callovian–Oxfordian red cherts and Rosso ad Aptici cherty marls at Colle di Sogno, Lombardy (Muttoni et al., 2005; Tables 1 and 2, entry #41), (ii) a coeval paleopole based on N = 25 characteristic magnetizations from the same stratigraphic interval from the nearby Torre de' Busi section (Channell et al., 2010; entry #42), and (iii) a more robust paleopole based on N = 54 characteristic magnetizations from Upper Oxfordian (~158 Ma) cherty limestones of the Fonzaso Formation at

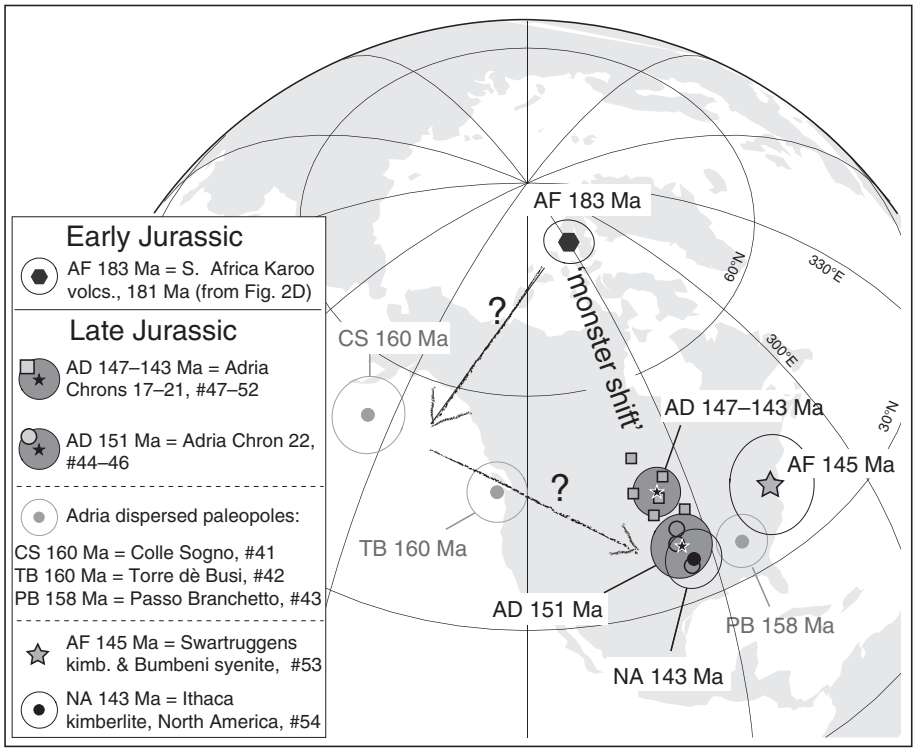

Fig. 3. Paleomagnetic poles corrected for inclination shallowing from parautochthonous Adria for the Late Jurassic compared with coeval poles from Africa (Swartruggens and Bumbeni) and North America (Ithaca); see Table 1 for paleopole entries (#) and text for discussion.

Passo del Branchetto, Veneto (Channell et al., 2010; entry #43). Paleopoles #41 from Colle di Sogno and #42 from Torre de' Busi were not corrected for inclination shallowing due to the limited number of paleomagnetic directions that define them, whereas the Passo del Branchetto paleopole (#43) yielded a flattening factor f = 0.72 (Supplementary Fig. 3G; Table 1). Inspection of Fig. 3 reveals that these single-site

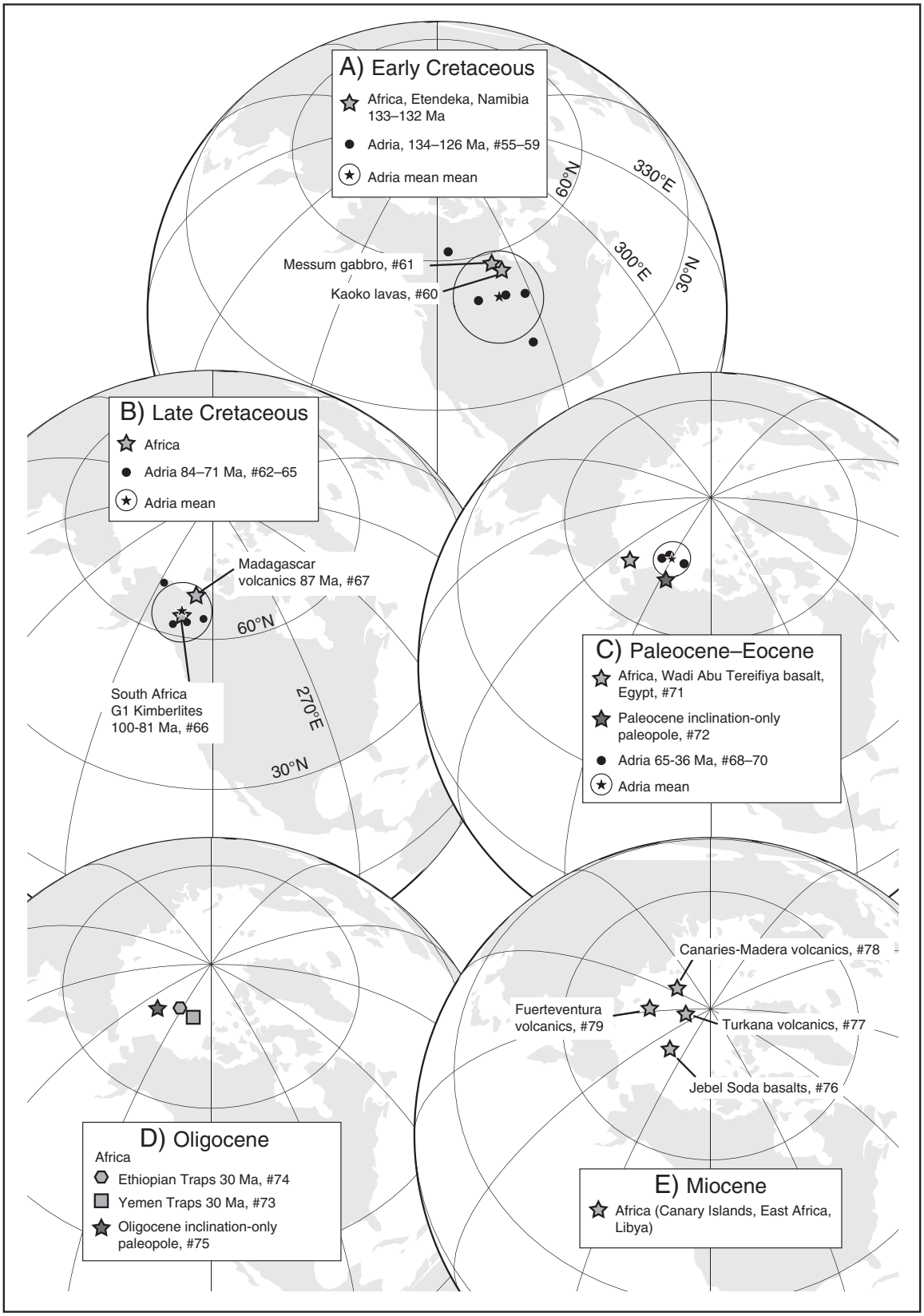

Fig. 4. Paleomagnetic poles corrected for inclination shallowing from parautochthonous Adria for the Early Cretaceous (A), Late Cretaceous (B), Paleocene–Eocene (C), Oligocene (D), and Miocene (E) compared with coeval poles from Africa; see Table 1 for paleopole entries (#) and text for discussion.

paleopoles (CS, TB, PB for entries #41, #42, and #43, respectively) are dispersed in apparent age progression along a swath of longitudes/latitudes from the northern Pacific to the southern U.S., with the ~158 Ma PB paleopole falling close to the ~151 Ma mean paleopole of Adria. We therefore infer that the polar 'monster shift' from ~183 Ma to ~151 Ma includes a (poorly resolved) cusp centered on the northern Pacific (Fig. 3) that actually explains the sub-equatorial paleolatitudes associated with deposition of radiolarian cherts typical of the Late Jurassic of Adria (Aiello and Hagstrum, 2001; Muttoni et al., 2005; see also Section 5).

3.7. Early Cretaceous

Early Cretaceous (Hauterivian–Barremian; ~134–126 Ma) data have been obtained from classic sections of the Maiolica Formation that have been used for the definition of all modern generations of geomagnetic polarity time scales; these sections are Capriolo from Lombardy (Channell et al., 1987; Table 1, entry #55), Cismon (outcrop section) from Veneto (Channell et al., 2000; #56), Polaveno and San Giovanni from Lombardy (Channell and Erba, 1992; #57 and #58), and Valle del Mis, Veneto (Channell et al., 1993; #59). We obtained flattening factors of f = 0.78 at Capriolo, f = 0.56 at Cismon outcrop section (data from the Cismon core section were not considered as the core was not oriented precisely during drilling; Channell et al., 2000), f = 0.82 at Polaveno, f = 0.94 at San Giovanni, and f = 0.86 at Valle del Mis (Supplementary Fig. 4). The corrected paleopoles are reasonably well clustered, and the overall mean paleopole that they yield is close to two key entries from igneous rocks from Africa: the paleomagnetic pole from the Etendeka Kaoko lavas from Namibia (Gidskehaug et al., 1975), and the paleopole from the Etendeka Messum gabbros from Namibia (Renne et al., 2002), both rotated to northwest Africa (=Adria) coordinates using the rotation parameters of Lottes and Rowley (1990) (Table 1, entries #60 and #61; Fig. 4A). The Kaoko lavas (dated to 128–110 Ma according to Gidskehaug et al., 1975) and the Messum gabbros (dated to ~133 Ma according to Renne et al., 2002) were emplaced during peak Etendeka magmatism at 133–132 Ma (Renne et al., 2002), making the agreement of these paleopoles with the ~134–126 Ma paleopole from Adria a strong argument in favor of Adria–Africa tectonic coherence at these times. We thus calculate a combined Adria–Africa overall mean paleopole with mean age of ~130 Ma in the Early Cretaceous (Table 2).

3.8. Late Cretaceous

Several paleomagnetic studies are available from classic sections of Late Cretaceous (Turonian–Maastrichtian; ~94–66 Ma) age encompassing the Scaglia Rossa Formation from the Southern Alps (Channell et al., 1992; Màrton et al., 2010) and the Istria and Gargano forelands of eastern and southeastern Adria (see references in Channell, 1996). We could not check for inclination shallowing at these sites/sections either because they comprise insufficient paleomagnetic directions to perform a statistically significant E/I test, or because the paleomagnetic directions are not available for testing. Hence, we focused on data from Late Cretaceous volcanic rocks from Sicily.

Four entries are listed in Table 1 (#62–65) from basalt flows at Capo Passero in the Hyblean foreland of southeastern Sicily (Schult, 1973; Barberi et al., 1974; Gregor et al., 1975; Grasso et al., 1983) and radiometrically dated to ~84–71 Ma and thus Campanian in age (Barberi et al., 1974). These paleomagnetic poles, assumed to be free from inclination shallowing, yield an overall mean paleopole that is consistent with two key entries from broadly coeval igneous rocks from Africa, namely the 100–81 Ma Group 1 Kimberlites from South Africa of Hargraves (1989; entry #66), and the ~87 Ma Madagascar volcanic rocks of Torsvik et al. (1998; entry #67) (Fig. 4B), allowing the calculation of a Cenomanian–Campanian (100–71 Ma) Adria–Africa overall mean paleomagnetic pole (Table 2).

3.9. Paleocene–Eocene

Several magnetostratigraphic and biostratigraphic studies have been conducted in recent years on expanded, continuous sections of Paleocene–Eocene age from the Belluno Basin of the Southern Alps. In our review, we include data from the Paleocene–Eocene South Ardo section (Dallanave et al., 2012; Table 1, entry #68), for which we obtained a flattening factor f = 0.6, the Paleocene–Eocene Cicogna section (Dallanave et al., 2009; entry #69), which yielded f = 0.41, and the Eocene Alano section (Agnini et al., 2011; entry #70) with f = 0.62 (Supplementary Fig. 5A, B, C). The corrected mean paleomagnetic pole calculated from these three entries agrees reasonably well with two paleopoles from Africa, the Wadi Abu Tereifiya volcanic rocks paleopole from Egypt, tentatively attributed to the Eocene (Hussain et al., 1979) (Table 1, entry #71; Fig. 4C), and the Paleocene paleopole of Schneider and Kent (1990) that is based on paleomagnetic inclination data from sediments at DSDP Site 524, ODP Site 707, and Gubbio (Italy), which define three colatitude small circles that intercept at one point (the paleopole) assuming no (0%) octupole (G3) contribution, and presumably also no significant inclination shallowing (Table 1, entry #72; Fig. 4C). These five entries have been used to calculate an overall mean Adria–Africa paleomagnetic pole valid for the Paleocene–Eocene, from 65 to 36 Ma (mean age of 50 Ma; Table 2).

3.10. Oligocene–Miocene

No reliable paleomagnetic data are available from Oligocene–Miocene rocks from parautochthonous Adria. Paleomagnetic poles from the Yemen Traps of the Arabian peninsula (Riisager et al., 2005; entry #73), rotated into northwest Africa using rotation parameters of Besse and Courtillot (2002), and the Ethiopian Traps from Ethiopia (Kidane et al., 2002; entry #74), pertain to the same large igneous province (LIP) dated at ~30 Ma (Riisager et al., 2005). These paleopoles plot close to the Oligocene paleopole of Schneider and Kent (1990) based on paleomagnetic inclination data from sediments at DSDP Site 523, ODP Site 706, and Gubbio (Italy), which define colatitude small-circles that intercept at the paleopole after assuming a 5% octupole (G3) contribution (Table 1, #75; Fig. 4D); this procedure of optimizing small-circle intersections by adopting an octupole field contribution of proper sign (Schneider and Kent, 1990) most likely removed any unrecognized sedimentary inclination flattening bias. The Oligocene data from the Yemen and Ethiopian Traps, and the G3-corrected entry from the African plate, are used to calculate an overall mean paleopole for Africa at ~28 Ma (Table 2).

Finally, for the Miocene we used paleomagnetic poles from the Jebel Soda alkali basalts of Libya (Schult and Soffel, 1973) dated to 16–8 Ma according to Bardintzeff et al. (2012) (Table 1, entry #76), the east African volcanic rocks dated to around 17 Ma (Reilly et al., 1976; entry #77), the Canary Islands and Madeira volcanic rocks with ages between 5.2 and 25 Ma (Watkins, 1973; entry #78), and the Fuerteventura volcanic rocks (lava series II) of Miocene–Pliocene age (Storetvedt et al., 1979; entry #79). These entries, used also in the apparent polar wander path of Tauxe et al. (1983), fall relatively close to each other (Fig. 4E) and define an overall mean high latitude paleopole for Africa with mean age of ~14 Ma (Table 2).

4. The Adria–Africa APWP

Our parautochthonous Adria–stable Africa composite APWP spans the Early Permian to Miocene (Table 2) and consists of two distinct tracks. From ~280 Ma to ~183 Ma, during Pangea time, paleopoles show a clockwise progression over North America from low to high latitudes, whereas from ~151 Ma to ~14 Ma, paleopoles show a second regular progression from low to high latitudes over North America. The ~151–130 Ma segment of our Adria–Africa APWP is broadly similar

in shape to the APWP recently derived from sedimentary successions from the central Apennines (Satolli et al., 2008). We plotted selected paleopoles of the Apennine APWP of Satolli et al. (2008) at 145 Ma, 141 Ma, 130 Ma, 116 Ma and 102 Ma for comparison with our Adria–Africa APWP (analysis not shown). We found that the Apennine paleopoles are variably displaced relative to our Adria–Africa paleopoles at 151 Ma, 145 Ma, and 130 Ma by about 24°–27° counter-clockwise due to Apennines deformation, and therefore, they have not been incorporated in our Adria–Africa data compilation. An earlier compilation of paleopoles from the central Apennines (Umbria) includes 8 sites from the Corniola Formation of Pliensbachian (~185 Ma) age and the Ammonitico Rosso of Toarcian–Aalenian (~177 Ma) age (Channell, 1992). After compensation of the originally-assumed 20° counter-clockwise rotation, the resulting mean pole position (67.7°N, 260.6°E) lies close to the Adria (Colle di Signo) pole for the Early Jurassic (Table 1, entry #36; Fig. 2D) and would be coincident with it if a slightly larger rotation (~25°) rotation were assumed.

The large magnitude pole shift of ~40° in the Adria–Africa APWP between ~183 Ma and ~151 Ma (Fig. 5A) is, therefore, supported by paleomagnetic data from the central Apennines (Channell, 1992; Satolli et al., 2008) although these data are not used in this paper to resolve it. On the other hand, the details of the path of this ~40° Jurassic pole-shift are poorly defined, with only three single-site paleopoles available from stable Adria (CS, TB, PB in Fig. 3 and Section 3.6) that are dispersed along a swath of longitudes/latitudes but are associated with a narrow range of ages (160–158 Ma, Fig. 3), and are provisionally not included in the composite Adria–Africa APWP (Fig. 5A; Table 2). It is during this major Jurassic pole shift that Adria attained sub-equatorial paleolatitudes consistent with the concurrent deposition of upwelling-related radiolarian cherts (Aiello and Hagstrum, 2001; Muttoni et al., 2005) and the carbonate platform productivity crisis due to eutrophication of parts of the Tethyan Ocean (Bartolini and Cecca, 1999).

A pole shift of similar magnitude — termed 'monster shift' — is present in the global APWP of Kent and Irving (2010), based on a compilation of inclination flattening-free paleomagnetic poles from North America and other continents, between the Early–Middle Jurassic (~190–160 Ma) paleopole standstill (= lack of significant polar movement), and the ~145 Ma mean paleopole obtained by averaging the Swartruggens and Bumbeni kimberlites paleopole of southern Africa (Hargraves et al., 1997), the Ithaca kimberlite paleopole of North America (Van Fossen and Kent, 1993), and the Hinlopenstretet dikes of Svalbard (Halvorsen, 1989) (see Kent and Irving, 2010 for further details).

We migrated the Kent and Irving (2010) (hereafter KI10) global APWP from North American to northwest Africa (= Adria) coordinates (Supplementary Table 1) and found a remarkable overall agreement between the 230, 200, 145, 130, 90, and 50 Ma paleopoles of the rotated KI10 APWP, and the 238, 201, 145, 130, 85, and 50 Ma paleopoles of our proposed Adria–Africa APWP (Fig. 5B). This agreement is regarded as significant, considering that the two curves represent substantially independent readings of the past positions of the Earth's spin axis, with only a moderate degree of redundancy in the Early Jurassic where both curves include paleopoles from the African CAMP and the Karoo LIP. The greatest discrepancy is observed between the ~183 Ma Adria–Africa paleopole, based entirely on Karoo LIP data, and the 190 and 180 Ma standstill paleopoles of the KI10 APWP (Fig. 5B), which are based on virtually the same data (~90% of shared paleopoles) with comparable mean ages (184.6 Ma and 182.3 Ma, respectively; Kent and Irving, 2010). Much of the observed discrepancy is accounted for by the incorporation in the 190–180 Ma KI10 paleopoles of five (out of a total of 8) paleopoles from igneous rocks (the White Mt. plutons of North America, the Garrawilla and Nombi volcanics and Tasmanian Dolerite of Australia, and the Marifil and Lepa-Osta Arena formations of South America; Kent and Irving, 2010) that, after rotation to northwest Africa coordinates (using rotation parameters listed in Kent and Irving, 2010), fall ~10–15° to the south of the Karoo LIP paleopole. We note that a high latitude for the ~183 Ma Adria–Africa paleopole is supported by the Ferrar Dolerite paleopole from Antarctica of Lanza and Zanella (1993) (also used in the KI10 APWP), which, after rotation to northwest Africa coordinates, falls at 71°N, 270°E, only ~8° away from the Karoo LIP paleopole.

Notwithstanding uncertainties in the position of the ~183 Ma Adria–Africa and ~180 Ma KI10 paleopoles, the remarkable agreement between the Adria–Africa and KI10 APWPs across the 'monster shift', especially its younger (~151–145 Ma) age limit (Fig. 5B), is not reproduced in other APWPs (e.g., Besse and Courtillot, 2003 [BC03]; Torsvik et al., 2008 [T08]; Torsvik et al., 2012 [T12]), after rotation to northwest Africa (= Adria) coordinates (Supplementary Table 1). The rapid polar shift observed in the Adria–Africa and KI10 APWPs (Fig. 5B) is not defined in the BC03 (Fig. 5C), T08 (Fig. 5D), and T12 (Fig. 5E) APWPs, which show broadly similar, smooth, and regular progressions of paleopoles over the Jurassic from northern latitudes at ~190 Ma to southern latitudes at 140 Ma. This discrepancy is probably caused by the fact that the ~160–140 Ma time window of the BC03, T08, and T12 APWPs is based on the time-averaging of paleopoles from Europe that are sparse, are not sufficiently well dated to define the rapid change in paleopoles of the APWP, and have complicated magnetizations (Muttoni et al., 2005; Kent and Irving, 2010). For example, the Jura Blue Limestone and Jura Mountains Oolites carry pre- and post-tectonic magnetizations, and the Sub-Tatric nappe sediments and Krakow Upland sediments are dominated by normal polarity magnetizations throughout a Middle–Late Jurassic time interval of high magnetic polarity reversal rates (see references to individual entries in Besse and Courtillot, 2002; Torsvik et al., 2008). A notable aspect of the T12 global APWP relative to the older T08 version is that in T12 an attempt is made to correct for sedimentary inclination shallowing by applying a blanket flattening factor of 0.6 to paleopole entries from sedimentary rocks (unless otherwise calculated by the original authors); however, we have seen in our compilation that the sedimentary flattening factor varies between 0.41 and 0.98 with a mean of 0.76 (Table 1).

The Jurassic 'monster shift' is identified in largely independent paleomagnetic datasets from different plates (North America, Adria–Africa), and it therefore represents a rapid event of contemporaneous plate motion with respect to the spin axis, which, according to Adria–Africa data, took place from ~183 Ma in the Early Jurassic to ~151 Ma in the Late Jurassic (or from the 190–160 Ma paleopole standstill to the 145 Ma paleopole according to Kent and Irving, 2010), and seems coincident with an episode of true polar wandering (TPW) recognized in the 195–145 Ma interval by Steinberger and Torsvik (2008). Invoking similarities between Eurasian (Pontides and Crimea) mid-Jurassic paleomagnetic data and coeval data from Adria of Muttoni et al. (2005), Meijers et al. (2010) also invoked TPW, considering it unlikely that Africa and Eurasia would have moved in close association relative to the surrounding plates at a time when Eurasia was bordered to the south by subducting slabs anchored in the mantle. Acknowledging that more data are required from non-Atlantic-bordering continents, we tentatively conclude that the rapid polar shift observed in Jurassic paleomagnetic data from North America, Adria–Africa, and Eurasia represent a major TPW event.

5. The role of paleolatitude on sedimentation

The Adria–Africa APWP can be used to estimate paleolatitudes for any given point of the African plate in order to gauge their influence on the overall distribution of climate-sensitive facies assuming a simple zonal climate distribution. To infer the latitudinal position of zonal climate belts in the past, we use the difference between precipitation and evaporation ($P - E$) based on the general circulation model of Manabe and Bryan (1985) with idealized geography (see also Kent and Muttoni, 2013). Although the model shows that the amplitude or climate severity of $P - E$ increases with increasing pCO_2 from

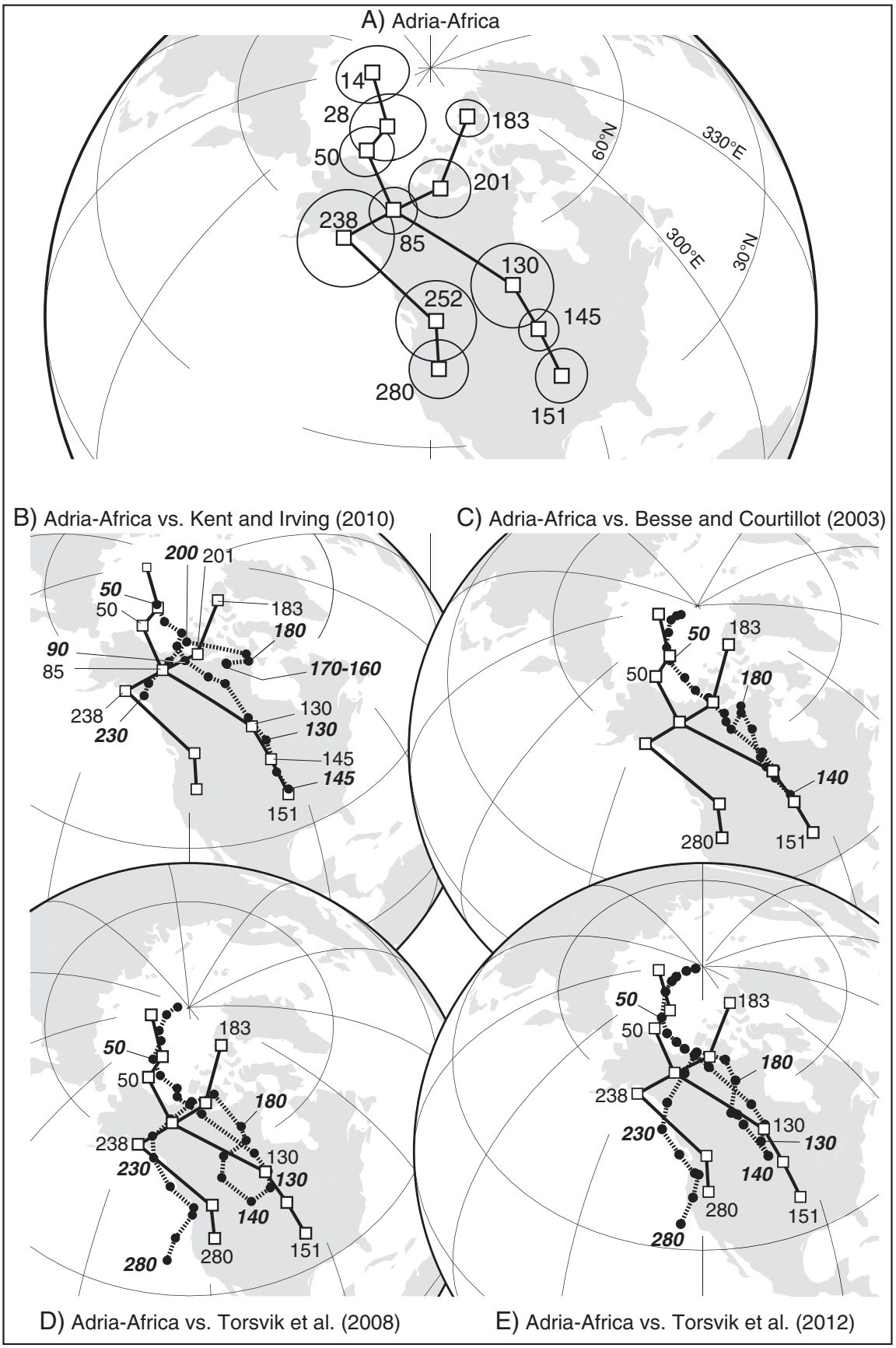

Fig. 5. The Adria–Africa apparent polar wander path (panel A; see Table 2 for mean paleomagnetic poles) compared with the apparent polar wander paths of Kent and Irving (2010) (B), Besse and Courtillot (2002, 2003) (C), Torsvik et al. (2008) (D), and Torsvik et al. (2012) (E), all rotated into northwest Africa (=Adria) coordinates (Supplementary Table 1). See text for discussion.

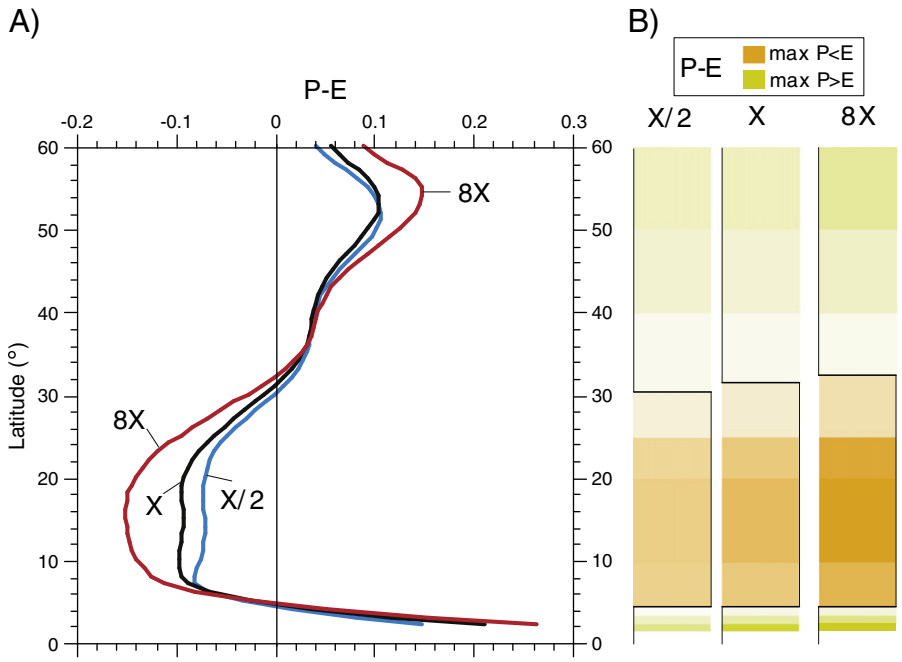

Fig. 6. In panel A, the latitudinal distribution of zonal indices of evaporation (E) *minus* precipitation (P) for atmospheric pCO_2 values ranging from one-half (X/2) to eight-fold (8X) pre-industrial level. In panel B, a color representation of the zonal E–P distribution showing a moderate (2–3°) contraction of the arid (P < E) tropical belt with lowering pCO_2. See text for discussion.
Panel A is redrawn from Manabe and Bryan (1985); see also Kent and Muttoni (2013).

one-half to 8-times the pre-industrial value (Fig. 6A), the latitudinal positions of the zonal boundaries where $P - E = 0$ tends to stay relatively fixed, within ~2–3° (Fig. 6B). We therefore set the equatorial humid belt where $P > E$ as occurring between 5°S and 5°N, the tropical arid belts ($P < E$) as extending from 5° to 30° latitude, and the temperate humid belts from 30° to the latitudinal limits of our paleolatitudinal reconstruction (Fig. 7).

The paleolatitude curve of northern Adria, calculated for a nominal point in the Southern Alps (Adamello Massif) (Fig. 7), shows a marked northward drift during the Permian–Triassic, reaching high northern latitudes by the time of emplacement of the Karoo LIP at ~183 Ma in the Early Jurassic. Then, the curve plummets to subequatorial latitudes during the ~183–151 Ma 'monster pole shift' and subsequently moves into tropical northern latitudes where it remains until ~50 Ma when a final northward progression restores the African plate to its modern location. To first order, as Adria (part of Pangea) drifted northward during the Permian–Triassic, the vertical sequence of climate sensitive facies in individual Tethyan basins changed as they passed from one climate belt to another. Fig. 7 shows that the interval between ~260 Ma in the Late Permian and ~205 Ma, close to the Norian–Rhaetian boundary, is characterized by Adria transiting across latitudes in the arid tropical belt from ~10°N to ~30°N when, on Adria and surrounding Tethyan realms, sediments of arid affinity were deposited in abundance. These arid sedimentary facies include the upper Permian fluvial deposits of the Verrucano Lombardo–Valgardena Sandstones (Cassinis and Perotti, 2007), the several Anisian–Norian shallow water carbonate platforms with coral build-ups from the southern Alps (e.g., Cernera Dolomite, Fois and Gaetani, 1984; Esino Limestone, Jadoul et al., 1992; Contrin Formation, Schlern/Sciliar Dolomite, Maurer, 2000; Dolomia Principale/Hauptdolomit, Jadoul et al., 2012), the Norian carbonate–evaporite platforms of the central-northern Apennines (Grezzoni Formation and Burano Anhydrite; Ciarapica, 2007), and the upper Olenekian–lower Anisian and Carnian evaporitic deposits of the Carniola di Bovegno and San Giovanni Bianco Formation of the southern Alps (Jadoul et al., 2012).

At ~205 Ma, when, according to our projection, northern Adria entered the mid-latitude humid belt (Fig. 7), a major change in depositional style occurred on Adria and surrounding Tethyan domains with the demise of carbonate productivity (end of Dolomia Principale/Hauptdolomit deposition in the southern Alps and of carbonate–evaporite deposition of the central-northern Apennines) and the onset of deposition of shale-rich successions (e.g. Riva di Solto Shale in the southern Alps, Kössen beds in Austria, Mt. Cetona Formation in the central-northern Apennines; Berra et al., 2010; Jadoul et al., 2012; Berra, 2012; Ciarapica, 2007). Further to the south on Adria, in the central-southern Apennines, the carbonate platforms continued to grow apparently without significant detrital influx (Ciarapica, 2007). However, a change in dolomitization is observed in the carbonate platforms of the southern Apennines whereby during the Norian, early dolomitization was intense and controlled by the occurrence of shallow, warm, and saline seawater, whereas the end Triassic (Rhaetian) and the Jurassic experienced a more humid climate during which early diagenetic dolomite formation was negligible (Iannace et al., 2011).

This shift from arid to humid climate has been recently interpreted as due to an equator-ward (southward) migration of the northern hemisphere humid temperate belt during a postulated Late Triassic glaciation that (1) exposed carbonate platforms to subaerial erosion forming terra-rossa paleosols and breccias, and (2) triggered the subsequent deposition of mudstones typical of more humid climates with higher rainfall rates (Berra et al., 2010; Berra, 2012). Indeed, the Manabe and Bryan (1985) circulation model predicts a contraction of the tropical arid belts by ~2–3°, accompanied by a parallel equator-ward migration of the temperate humid belts, with pCO_2 diminishing from 8-times to one-half the pre-industrial value (Fig. 6B). Moreover, climate simulations incorporating the northward drift of Pangea during the Late Triassic suggest significantly diminished greenhouse conditions with pCO_2 declining from more than 3000 ppm in the Carnian to less than 1000 ppm in the Rhaetian (Godderis et al., 2008). However, the tropical contraction model advocated by Berra (2012) to explain platform erosion followed by mudstone deposition requires the existence of a

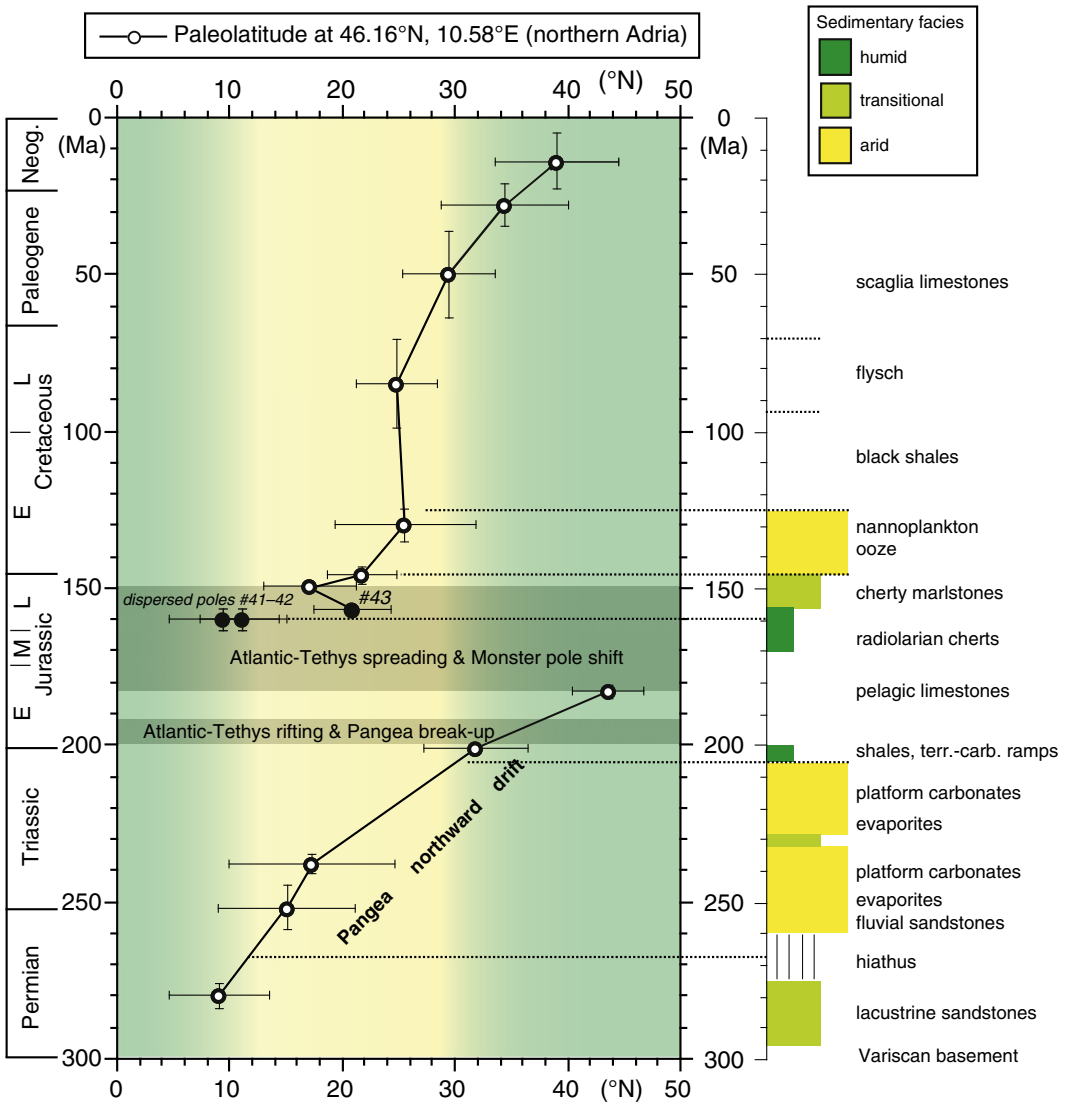

Fig. 7. The paleolatitudinal evolution of a nominal point in the Southern Alps of northern Adria (Adamello massif) calculated from the flattening-free Adria–Africa apparent polar wander path of Table 2 (white circles with error bars), showing the pronounced northward drift of Pangea during the Permian–Triassic and the 'monster pole shift' during Central Atlantic–Alpine Tethys spreading and Pangea break-up in the Jurassic. The details of the Jurassic 'monster pole shift' are poorly defined, with only three single-site, dispersed paleopoles available from Adria (entries #41–43 in Table 1), which have not been used to compute the Adria–Africa APWP of this study (Table 2) but that are here used to illustrate that during the Jurassic 'monster pole shift', Adria–Africa attained sub-equatorial paleolatitudes (black circles) conductive to the deposition of radiolarites (Muttoni et al., 2005). The latitudinal distribution of zonal climate belts based on models of evaporation (E) *minus* precipitation (P) (from Fig. 6), and a generalized summary of latitude-dependent Permian–Cenozoic sedimentary facies of northern-central Adria, are also plotted; see text for discussion.

discrete glacioeustatic event in the latest Norian, for which there is no sound evidence. As an alternative and simpler scenario, the demise of carbonate productivity and onset of mudstone deposition was triggered by the crossing of the arid–humid belt boundary centered on ~30°N as Adria, attached to Pangea, moved northward at speeds of ~0.45° latitude per Myr, passing a (focused) zonal belt boundary in less than 1 Myr (Fig. 7). In our model, the formation of terra-rossa paleosols and breccias at the top of Norian carbonate platforms resulted from the demise of carbonate productivity coupled with an accelerated hydrologic cycle conducive to erosion and weathering typical of mid-latitude humid climates.

As a consequence of the fragmentation of Pangea and opening of the Atlantic Ocean, Upper Triassic shallow-water sediments were replaced by mainly pelagic limestones in the Early Jurassic, radiolarian cherts in the Middle–Late Jurassic, and again pelagic limestones in the Late Jurassic–Cretaceous (Fig. 7). Previous analysis of paleolatitudinal data from a continuous succession of sediments from the Lombardian basin (Muttoni et al., 2005) showed that carbonate facies dominated when Adria was located at tropical latitudes in the Early Jurassic, radiolarian oozes were deposited when it moved to near-equatorial latitudes in the Middle–Late Jurassic, and nannofossil oozes became progressively dominant when it returned to higher tropical latitudes in the Late Jurassic–Cretaceous (Muttoni et al., 2005). Our analysis, which incorporates data of Muttoni et al. (2005) from the radiolarian cherts and overlying basal Rosso ad Aptici cherty marlstones (that define the CS paleopole of entry #41), shows that the sub-equatorial latitudes consistent with radiolarian ooze deposition occurred during the 'monster pole shift' from ~183 Ma to ~151 Ma. At broadly this time, several carbonate platforms experienced biodiversity loss, absence of deposition in hiatuses, and productivity crisis due to increased eutrophication of this part of the Tethyan Ocean (Bartolini and Cecca, 1999) that we believe was associated with subequatorial latitudes (Muttoni et al., 2005). In addition, Wiedenmayer (1980) refers to a "revolution" in central Mediterranean (Adria) ammonite fauna

immediately after the Pliensbachian–Toarcian boundary (~183 Ma) that may be a response to abrupt latitudinal change at this time. The subsequent deposition of the nannofossil oozes of the Maiolica Formation occurred when Adria returned to tropical latitudes of ~20–25°N in the latest Jurassic–Cretaceous (Fig. 7).

Although short-term climate change like the so-called Carnian Pluvial Event, which was recently associated with rapid emplacement of the Wrangellia LIP (Dal Corso et al., 2012), or the high frequency monsoon variability observed in the Triassic of Pangea (Mutti and Weissert, 1995), are not taken into account in our simple zonal climate model, we have shown that much of the overall architecture of the Mesozoic sedimentary succession of Adria can be explained using the "plate-stratigraphy" concept of Berger and Winterer (1974) based on continents drifting across standard zonal climate belts.

6. Conclusions

1. We examined a series of independent paleomagnetic mean directions from regions of Adria considered parautochthonous relative to the African craton, spanning from the Early Permian to the Eocene. Paleomagnetic data were obtained either from biostratigraphically dated sedimentary rocks that have been systematically corrected for inclination shallowing or from radiometrically dated igneous rocks that are considered free from inclination flattening.
2. Flattening-corrected and flattening-free paleomagnetic directions from parautochthonous Adria were used to calculate paleomagnetic poles for comparison with coeval paleopoles from Africa, again calculated from flattening-corrected or flattening-free data from sedimentary or igneous rocks, respectively.
3. Paleomagnetic poles from parautochthonous Adria and stable Africa are essentially coherent for several time slices from the Early Permian to the Eocene. The African affinity of paleopoles from Adria has been previously observed in data from the central Apennines (Channell, 1992; Satolli et al., 2007, 2008), however, paleopoles from the Apennines have not been included in the present compilation because they are variably rotated relative to the parautochthonous Adria paleopoles by as much as 24–27° counter-clockwise. On the other hand, compensation for central Apennine (Umbrian) tectonic rotation provides support for the composite Adria–Africa APWP, including the Early Jurassic 'monster shift' (point #5 below).
4. A composite APWP valid for parautochthonous Adria and stable Africa and extending from the Early Permian to the Miocene has been constructed for comparison with APWPs from the literature rotated into northwest Africa (= Adria) coordinates using standard rotation parameters. Particularly good visual agreement exists with the global APWP of Kent and Irving (2010) constructed from flattening-free paleomagnetic poles that are largely independent of (different from) poles used in our Adria–Africa APWP construction.
5. Both the Kent and Irving (2010) and our Adria–Africa APWPs show a major pole shift in the Jurassic (from ~183 Ma to ~151 Ma according to Adria–Africa data) that other APWPs (Besse and Courtillot, 2002, 2003; Torsvik et al., 2008; Torsvik et al., 2012) tend to underestimate — we surmise — because of time-averaging of data affected by remagnetizations. Considering that this Jurassic 'monster shift' was observed in independent paleomagnetic datasets from different plates (North America, Adria–Africa, Eurasia; Kent and Irving, 2010; Meijers et al., 2010; this study), it is considered evidence for a major, and previously largely unrecognized, TPW event that awaits confirmation from non-Atlantic bordering continents.
6. The composite Adria–Africa APWP provides estimates of paleolatitudes of northern Adria in order to gauge their potential control on Tethyan facies deposition under the assumption of simple zonal climate. We found that during the Triassic–Early Jurassic, Adria (attached to Pangea) moved northward at speeds of ~0.45° latitude per Myr, crossing the entire span of the northern hemisphere arid belt (~5–30°N) before entering the mid latitude humid belt. This drift motion across contrasting zonal climate belts determined the main architecture of the Mesozoic sedimentary succession of Adria. For example, widespread shallow-water carbonate platforms frequently associated with sabkha or evaporitic sediments characterize the Middle–Late Triassic when Adria moved across the tropical arid belt, while the demise of carbonate productivity at around the Norian–Rhaetian boundary occurred when northern-central Adria crossed the arid-humid zonal boundary at ~30°N.
7. Despite geologic complexities of the Adria–Africa connection (e.g., Speranza et al., 2012), our well-dated composite Adria–Africa APWP can be regarded as a useful ancillary curve to describe the last 280 million years of motion of the African continent.

Supplementary data to this article can be found online at http://dx.doi.org/10.1016/j.palaeo.2013.06.011.

Acknowledgments

John Geissman and Fabio Speranza are warmly thanked for useful reviews. Robert Scholger is thanked for providing a digital listing of the Bulla data. Luca Lanci, Fabrizio Berra and Dennis V. Kent are thanked for insightful comments on earlier versions of this manuscript. Research partly supported through NSF grant EAR-0337102 (to JC).

References

Agnini, C., Fornaciari, E., Giusberti, L., Grandesso, P., Lanci, L., Luciani, V., Muttoni, G., Palike, H., Rio, D., Spofforth, D.J.A., 2011. Integrated biomagnetostratigraphy of the Alano section (NE Italy): a proposal for defining the middle–late Eocene boundary. Geological Society of America Bulletin 123, 841–872.

Aiello, I.W., Hagstrum, J.T., 2001. Paleomagnetism and paleogeography of Jurassic radiolarian cherts from the northern Apennines of Italy. Geological Society of America Bulletin 113, 469–481.

Angiolini, L., Crippa, G., Muttoni, G., Pignatti, J., 2013. Guadalupian (Middle Permian) paleobiogeography of the Neotethys Ocean. Gondwana Research 24, 173–184.

Aubele, K., Bachtadse, V., Muttoni, G., Ronchi, A., Durand, M., 2012. A paleomagnetic study of Permian and Triassic rocks from the Toulon–Cuers Basin, SE France: evidence for intra-Pangea block rotations in the Permian. Tectonics 31, TC3015.

Bachtadse, V., Zanglein, R., Tait, J., Soffel, H., 2002. Palaeomagnetism of the Permo/Carboniferous (280 Ma) Jebel Nehoud ring complex, Kordofan, Central Sudan. Journal of African Earth Sciences 35, 89–97.

Barberi, F., Civetta, L., Gasparini, P., Innocenti, F., Scandone, R., Villari, L., 1974. Evolution of a section of the Africa–Europe plate boundary: paleomagnetic and volcanological evidence from Sicily. Earth and Planetary Science Letters 22, 123–132.

Bardintzeff, J.M., Deniel, C., Guillou, H., Platevoet, B., Telouk, P., Oun, K.M., 2012. Miocene to recent alkaline volcanism between Al Haruj and Waw an Namous (southern Libya). International Journal of Earth Sciences 101, 1047–1063.

Bartolini, A., Cecca, F., 1999. 20 My hiatus in the Jurassic of Umbria–Marche Apennines (Italy): carbonate crisis due to eutrophication. Comptes Rendus de l'Academie des Sciences Series IIA Earth and Planetary Science 329, 587–595.

Becke, M., Mauritsch, H.J., 1984. Rock and paleomagnetic investigations on the Quartz-porphyry Complex near Bolzano (Bozen), Italy. IGCP, Newsletter 6, 11–19.

Berger, W.H., Winterer, E.L., 1974. Plate stratigraphy and the fluctuating carbonate line. In: Hsu, K.J., Jenkins, H.C. (Eds.), Pelagic Sediments: On Land and Under the Sea. Blackwell Scientific Publications, Oxford, pp. 11–48.

Berra, F., 2012. Sea-level fall, carbonate production, rainy days: how do they relate? Insight from Triassic carbonate platforms (Western Tethys, Southern Alps, Italy). Geology 40, 271–274.

Berra, F., Jadoul, F., Anelli, A., 2010. Environmental control on the end of the Dolomia Principale/Hauptdolomit depositional system in the central Alps: coupling sea-level and climate changes. Palaeogeography, Palaeoclimatology, Palaeoecology 290, 138–150.

Besse, J., Courtillot, V., 2002. Apparent and true polar wander and the geometry of the geomagnetic field over the last 200 Myr. Journal of Geophysical Research 107, 2300. http://dx.doi.org/10.1029/2000JB000050.

Besse, J., Courtillot, V., 2003. Correction to "Apparent and true polar wander and the geometry of the geomagnetic field over the last 200 Myr". Journal of Geophysical Research 108 (B10), 2469. http://dx.doi.org/10.1029/2003JB002684.

Brack, P., Mundil, R., Oberli, F., Meier, M., Rieber, H., 1996. Biostratigraphic and radiometric age data question the Milankovitch characteristics of the Latemar cycles (Southern Alps). Geology 24, 371–375.

Brack, P., Muttoni, G., 2000. High-resolution magnetostratigraphic and lithostratigraphic correlations in Middle Triassic pelagic carbonates from the Dolomites (northern Italy). Palaeogeography, Palaeoclimatology, Palaeoecology 161, 361–380.

Brack, P., Muttoni, G., Rieber, H., 2001. Comment on: "Magnetostratigraphy and biostratigraphy of the Middle Triassic Margon section (Southern Alps, Italy" by P.R. Gialanella, F. Heller, P. Mietto, A. Incoronato, V. De Zanche, P. Gianolla, G. Roghi [Earth Planet. Sci. Lett. 187 (2001) 17–25]. Earth and Planetary Science Letters 193, 253–255.

Brack, P., Rlieber, H., Nicora, A., Mundil, R., 2005. The Global Boundary Stratotype Section and Point (GSSP) of the Ladinian Stage (Middle Triassic) at Bagolino (Southern Alps, Northern Italy) and its implications for the Triassic time scale. Episodes 28, 233–244.

Broglio Loriga, C., Cirilli, S., De Zanche, V., di Bari, D., Gianolla, P., Laghi, G.F., Lowrie, W., Manfrin, S., Mastandrea, A., Mietto, P., Muttoni, G., Neri, C., Posenato, P., Rechichi, M., Rettori, R., Roghi, G., 1999. The Prati di Stuores/Stuores Wiesen section (Dolomites, Italy): a candidate Global Stratotype Section and Point for the base of the Carnian stage. Rivista Italiana di Paleontologia e Stratigrafia 105, 37–78.

Carrapa, B., Bertotti, G., Krijgsman, W., 2003. Subsidence, stress regime and rotation(s) of a tectonically active sedimentary basin within the Western Alpine Orogen: the tertiary Piedmont Basin (Alpine Domain, NW Italy). Geological Society Special Publication 208, 205–227.

Cassinis, G., Perotti, C., 2007. A stratigraphic and tectonic review of the Italian Southern Alpine Permian. Palaeoworld 16, 140–172.

Castellarin, A., Cantelli, L., Fesce, A.M., Mercier, J.L., Picotti, V., Pini, G.A., Prosser, G., Selli, L., 1992. Alpine compressional tectonics in the Southern Alps. Relationships with the N-Apennines. Annales Tectonicae 6, 62–94.

Channell, J.E.T., Tarling, D.H., 1975. Palaeomagnetism and the rotation of Italy. Earth and Planetary Science Letters 25, 177–188.

Channell, J.E.T., Lowrie, W., Medizza, F., Alvarez, W., 1978. Palaeomagnetism and tectonics in Umbria, Italy. Earth and Planetary Science Letters 39, 199–210.

Channell, J.E.T., D'Argenio, B., Horvath, F., 1979. Adria, the African Promontory, in Mesozoic Mediterranean paleogeography. Earth-Science Reviews 15, 213–292.

Channell, J., Bralower, T., Grandesso, P., 1987. Biostratigraphic correlation of Mesozoic polarity chrons CM1 to CM23 at Capriolo and Xausa (Southern Alps, Italy). Earth and Planetary Science Letters 85, 203–221.

Channell, J.E.T., Oldow, J., Catalano, R., d'Argenio, B., 1990. Paleomagnetically determined rotations in the western Sicilian fold and thrust belt. Tectonics 9, 641–660.

Channell, J.E.T., 1992. Paleomagnetic data from Umbria (Italy): implications for the rotation of Adria and Mesozoic apparent polar wander paths. Tectonophysics 216, 365–378.

Channell, J.E.T., Doglioni, C., Stoner, J.S., 1992. Jurassic and Cretaceous paleomagnetic data from the Southern Alps (Italy). Tectonics 11, 811–822.

Channell, J.E.T., Erba, E., 1992. Early Cretaceous polarity chrons CM0 to CM11 recorded in northern Italian land sections near Brescia. Earth and Planetary Science Letters 108, 161–179.

Channell, J.E.T., Erba, E., Lini, A., 1993. Magnetostratigraphic calibration of the Late Valanginian carbon isotope event in pelagic limestones from Northern Italy and Switzerland. Earth and Planetary Science Letters 118, 145–166.

Channell, J.E.T., Doglioni, C., 1994. Early Triassic paleomagnetic data from the Dolomites (Italy). Tectonics 13, 157–166.

Channell, J.E.T., 1996. Palaeomagnetism and palaeogeography of Adria. In: Morris, A., Tarling, D.H. (Eds.), Palaeomagnetism and Tectonics of the Mediterranean Region. Geological Society Special Publication, London, pp. 119–132.

Channell, J.E.T., Erba, E., Muttoni, G., Tremolada, F., 2000. Early Cretaceous magnetic stratigraphy in the APTICORE drill core and adjacent outcrop at Cismon (Southern Alps, Italy), and correlation to the proposed Barremian–Aptian boundary stratotype. Geological Society of America Bulletin 112, 1430–1443.

Channell, J.E.T., Casellato, C., Muttoni, G., Erba, E., 2010. Magnetostratigraphy, nannofossil stratigraphy and apparent polar wander for Adria–Africa in the Jurassic–Cretaceous boundary interval. Palaeogeography, Palaeoclimatology, Palaeoecology 293, 51–75.

Ciarapica, G., 2007. Regional and global changes around the Triassic–Jurassic boundary reflected in the late Norian–Hettangian history of the Apennine basins. Palaeogeography, Palaeoclimatology, Palaeoecology 244, 34–51.

Clark, D., Lackie, M., 2003. Palaeomagnetism of the Early Permian Mount Leyshon intrusive complex and Tuckers igneous complex, North Queensland, Australia. Geophysical Journal International 153, 523–547.

Courtillot, V.E., Renne, P.R., 2003. On the ages of flood basalt events. Comptes Rendus Geosciences 335, 113–140.

Dal Corso, J., Mietto, P., Newton, R.J., Pancost, R.D., Preto, N., Roghi, G., Wignall, P.B., 2012. Discovery of a major negative $\delta^{13}C$ spike in the Carnian (Late Triassic) linked to the eruption of Wrangellia flood basalts. Geology 40, 79–82.

Dallanave, E., Agnini, C., Muttoni, G., Rio, D., 2009. Magneto-biostratigraphy of the Cicogna section (Italy): implications for the late Paleocene,Äìearly Eocene time scale. Earth and Planetary Science Letters 285, 39–51.

Dallanave, E., Agnini, C., Muttoni, G., Rio, D., 2012. Paleocene magneto-biostratigraphy and climate-controlled rock magnetism from the Belluno Basin, Tethys Ocean, Italy. Palaeogeography, Palaeoclimatology, Palaeoecology 337–338, 130–142.

Dalrymple, G.B., Gromme, C.S., White, R.W., 1975. Potassium–argon age and paleomagnetism of diabase dikes in Liberia: initiation of central Atlantic rifting. Geological Society of America Bulletin 86, 399–411.

Daly, L., Pozzi, J.-P., 1976. Resultats paleomagnetiques du Permien inferieur et du Trias Marocain; comparaison avec les Donnees Africaines et Sud Americaines. Earth and Planetary Science Letters 29, 71–80.

DeKock, M., Kirschvink, J., 2004. Paleomagnetic constraints on the Permian–Triassic Boundary in terrestrial strata of the Karoo Supergroup, South Africa: implications for causes of the End-Permian extinction event. Gondwana Research 7, 175–183.

Dewey, J.F., Helman, M.L., Turco, E., Hutton, D.H.W., Knott, S.D., 1989. Kinematics of the western Mediterranean. In: Cowoard, M.P., Dietrich, D., Park, R.G. (Eds.), Alpine Tectonics. Geological Society, London, pp. 265–283.

Domeier, M., Van der Voo, R., Torsvik, T.H., 2011a. Paleomagnetism and Pangea: the road to reconciliation. Tectonophysics 514–517, 14–43.

Domeier, M., Van der Voo, R., Tohver, E., Tomezzoli, R.N., Vizan, H., Torsvik, T.H., Kirshner, J., 2011b. New Late Permian paleomagnetic data from Argentina: refinement of the apparent polar wander path of Gondwana. Geochemistry, Geophysics, Geosystems 12, Q07002.

Fois, E., Gaetani, M., 1984. The recovery of reef-building communities and the role of cnidarians in carbonate sequences of the Middle Triassic (Anisian) in the Italian Dolomites. Palaeontographica Americana 54, 191–200.

Font, E., Youbi, N., Fernandes, S., El Hachimi, H., Kratinova, Z., Hamim, Y., 2011. Revisiting the magnetostratigraphy of the Central Atlantic Magmatic Province (CAMP) in Morocco. Earth and Planetary Science Letters 309, 302–317.

Gialanella, P.R., Heller, F., Mietto, P., Incoronato, A., De Zanche, V., Gianolla, P., Roghi, G., 2001. Magnetostratigraphy and biostratigraphy of the Middle Triassic Margon section (Southern Alps, Italy). Earth and Planetary Science Letters 187, 17–25.

Gidskehaug, A., Creer, K.M., Mitchell, J.G., 1975. Palaeomagnetism and K–Ar ages of the south-west African basalts and their bearing on the time of initial rifting of the South Atlantic Ocean. Geophysical Journal of the Royal Astronomical Society 42, 1–20.

Godderis, Y., Donnadieu, Y., De Vargas, C., Pierrehumbert, R.T., Dromart, G., Van De Schootbrugge, B., 2008. Causal or casual link between the rise of nannoplankton calcification and a tectonically-driven massive decrease in Late Triassic atmospheric CO_2? Earth and Planetary Science Letters 267, 247–255.

Gradstein, F.M., Ogg, J.G., Schmitz, M.D., Ogg, G.M., 2012. The Geologic Time Scale. Elsevier, Boston 1144.

Grasso, M., Lentini, F., Nairn, A.E.M., Vigliotti, L., 1983. A geological and paleomagnetic study of the Hyblean Volcanic Rocks, Sicily. Tectonophysics 93, 271–295.

Gregor, C., Nairn, A.E.M., Negendank, J.F.W., 1975. Paleomagnetic investigations of the tertiary and quaternary rocks: IX The pliocene of southeast Sicily and some Cretaceous rocks from Capo Passero. Geologische Rundschau 64, 948–958.

Hailwood, E., Mitchell, J., 1971. Palaeomagnetic and radiometric dating results from Jurassic intrusions in South Morocco. Geophysical Journal of the Royal Astronomical Society 24, 351–364.

Halvorsen, E., 1989. A paleomagnetic pole position of Late Jurassic/Early Cretaceous dolerites from Hinlopenstretet, Svalbard, and its tectonic implications. Earth and Planetary Science Letters 94, 398–408.

Hargraves, R.B., 1989. Paleomagnetism of Mesozoic kimberlites in southern Africa and the Cretaceous apparent polar wander curve for Africa. Journal of Geophysical Research 94, 1851–1866.

Hargraves, R., Rehacek, J., Hooper, P., 1997. Palaeomagnetism of the Karoo igneous rocks in southern Africa. South African Journal of Geology 100, 195–212.

Hargraves, R.B., Briden, J.C., Daniels, B.A., 1999. Palaeomagnetism and magnetic fabric in the Freetown Complex, Sierra Leone. Geophysical Journal International 136, 705–713.

Heiniger, C., 1979. Paleomagnetic and rock magnetic properties of the Permian volcanics in the western Southern Alps. Journal of Geophysics 46, 397–411.

Heller, F., Lowrie, W., Hirt, A.M., 1989. A review of palaeomagnetic and magnetic anisotropy results from the Alps. In: Cowar, M.P., Dietrich, D., Park, R.G. (Eds.), Alpine Tectonics. Geological Society Special Publication, pp. 399–420.

Hirt, A.M., Lowrie, W., 1988. Paleomagnetism of the Umbrian–Marches orogenic belt. Tectonophysics 146, 91–103.

Hounslow, M.W., Muttoni, G., 2010. The geomagnetic polarity timescale for the Triassic: linkage to stage boundary definitions. Geological Society, London, Special Publications 334, 61–102.

Hussain, A.G., Schult, A., Soffel, H., 1979. Paleomagnetism of basalts of Wadi Abu Tereifiya, Mandisha and dioritic dikes of Wadi Abu Shihat, Egypt. Geophysical Journal of the Royal Astronomical Society 56, 55–61.

Iannace, A., Capuano, M., Galluccio, L., 2011. 'Dolomites and dolomites' in Mesozoic platform carbonates of the Southern Apennines: geometric distribution, petrography and geochemistry. Palaeogeography, Palaeoclimatology, Palaeoecology 310, 324–339.

Irving, E., 1977. Drift of the major continental blocks since the Devonian. Nature 270, 304–309.

Jadoul, F., Gervasutti, M., Fantini Sestini, N., 1992. The Middle Triassic of the Brembana Valley: preliminary study of the Esino platform (Bergamasc Alps). Rivista Italiana di Paleontologia e Stratigrafia 98, 299–324.

Jadoul, F., Galli, M.T., Muttoni, G., Rigo, M., Cirilli, S., 2012. The late Norian–Hettangian stratigraphic and paleogeographic evolution of the Bergamasc Alps. Geological Field Trip 4, 1–55. http://dx.doi.org/10.3301/GFT.2012.01.

Kent, D.V., Tauxe, L., 2005. Corrected Late Triassic latitudes for continents adjacent to the North Atlantic. Science 307, 240–244.

Kent, D.V., Irving, E., 2010. Influence of inclination error in sedimentary rocks on the Triassic and Jurassic apparent polar wander path for North America and implications for Cordilleran tectonics. Journal of Geophysical Research 115, B10103. http://dx.doi.org/10.1029/2009JB007205.

Kent, D.V., Muttoni, G., 2013. Modulation of Late Cretaceous and Cenozoic climate by variable drawdown of atmospheric pCO_2 from weathering of basaltic provinces on continents drifting through the equatorial humid belt. Climate of the Past 9, 525–546.

Kidane, T., Abebe, B., Courtillot, V., Herrero, E., 2002. New paleomagnetic result from the Ethiopian flood basalts in the Abbay (Blue Nile) and Kessem gorges. Earth and Planetary Science Letters 203, 353–367.

King, R.F., 1955. The remanent magnetism of artificially deposited sediment. Monthly Notices Royal Astronomical Society, Geophysics Supplement 7, 115–134.

Kipfer, R., Heller, F., 1988. Palaeomagnetism of Permian red beds in the contact aureole of the Tertiary Adamello intrusion (northern Italy). Physics of the Earth and Planetary Interiors 52, 365–375.

Klitgord, K.D., Schouten, H., 1986. Plate kinematics of the central Atlantic. In: Tucholke, B.E., Vogt, P.R. (Eds.), The Geology of North America. The Western North Atlantic Region. Geological Society of America, Boulder, CO, pp. 351–378.

Kosterov, A.A., Perrin, M., 1996. Paleomagnetism of the Lesotho basalt, southern Africa. Earth and Planetary Science Letters 139, 63–78.
Jourdan, F., Feraud, G., Bertrand, H., Kampunzu, A.B., Tshoso, G., Watkeys, M.K., Le Gall, B., 2005. Karoo large igneous province: brevity, origin, and relation to mass extinction questioned by new $^{40}Ar/^{39}Ar$ age data. Geology 33, 745–748.
Lanci, L., Tohver, E., Wilson, A., Flint, S., 2013. Upper Permian magnetic stratigraphy of the lower Beaufort group, Karoo basin. Earth and Planetary Science Letters. http://dx.doi.org/10.1016/j.epsl.2013.05.017 (in press).
Lanza, R., Zanella, E., 1993. Palaeomagnetism of the Ferrar Dolerite in the northern Prince Albert Mountains (Victoria Land, Antarctica). Geophysical Journal International 114, 501–511.
Lottes, A.L., Rowley, D.B., 1990. Reconstruction of the Laurasian and Gondwanan segments of Permian Pangaea. In: McKerrow, W.S., Scotese, C.R. (Eds.), Palaeozoic Palaeogeography and Biogeography. Geological Society of America, pp. 383–395.
Lowrie, W., Alvarez, W., 1975. Paleomagnetic evidence for the rotation of the Italian Peninsula. Journal of Geophysical Research 80, 1579–1592.
Manabe, S., Bryan, K., 1985. CO_2-induced change in a coupled ocean–atmosphere model and its paleoclimatic implications. Journal of Geophysical Research 90, 11689–11707.
Manzoni, M., 1970. Paleomagnetic data of Middle and Upper Triassic age from the Dolomites (eastern Alps, Italy). Tectonophysics 10, 411–424.
Màrton, E., Zampieri, D., Grandesso, P., Cosovic, V., Moro, A., 2010. New Cretaceous paleomagnetic results from the foreland of the Southern Alps and the refined apparent polar wander path for stable Adria. Tectonophysics 480, 57–72.
Meijers, M.J.M., Langereis, C.G., van Hinsbergen, D.J.J., Kaymakci, N., Stephenson, R.A., Altiner, D., 2010. Jurassic–Cretaceous low paleolatitudes from the circum-Black Sea region (Crimea and Pontides) due to True Polar Wander. Earth and Planetary Science Letters 296, 210–226.
Maffione, M., Speranza, F., Faccenna, C., Cascella, A., Vignaroli, G., Sagnotti, L., 2008. A synchronous Alpine and Corsica–Sardinia rotation. Journal of Geophysical Research 113, B03104. http://dx.doi.org/10.1029/2007JB005214.
Mattei, M., Kissel, C., Funiciello, R., 1996. No tectonic rotation of the Tuscan Tyrrhenian margin (Italy) since late Messinian. Journal of Geophysical Research 101, 2835–2845.
Maurer, F., 2000. Growth mode of middle Triassic carbonate platforms in the western Dolomites (Southern Alps, Italy). Sedimentary Geology 134, 275–286.
Mietto, P., Manfrin, S., Preto, N., Rigo, M., Roghi, G., Furin, S., Gianolla, P., Posenato, R., Muttoni, G., Nicora, A., Buratti, N., Cirilli, S., Spötl, C., Ramezani, J., Bowring, S.A., 2012. The Global Boundary Stratotype Section and Point (GSSP) of the Carnian stage (Late Triassic) at Prati di Stuores/Stuores Wiesen section (Southern Alps, NE Italy). Episodes 35, 414–430.
Moulin, M., Fluteau, F., Courtillot, V., Marsh, J., Delpech, G., Quidelleur, X., Gerard, M., Jay, A.E., 2011. An attempt to constrain the age, duration, and eruptive history of the Karoo flood basalt: Naude's Nek section (South Africa). Journal of Geophysical Research 116, B07403.
Mundil, R., Brack, P., Meier, M., Rieber, H., Oberli, F., 1996. High-resolution U–Pb dating of Middle Triassic volcaniclastics: time-scale calibration and verification of tuning parameters for carbonate sedimentation. Earth and Planetary Science Letters 141, 137–151.
Mutti, M., Weissert, H., 1995. Triassic monsoonal climate and its signature in Ladinian–Carnian carbonate platforms (Southern Alps, Italy). Journal of Sedimentary Research 65B, 357–367.
Muttoni, G., Kent, D.V., Channell, J.E.T., 1996. Evolution of Pangea: paleomagnetic constraints from the Southern Alps, Italy. Earth and Planetary Science Letters 140, 97–112.
Muttoni, G., Kent, D.V., Brack, P., Nicora, A., Balini, M., 1997. Middle Triassic magneto-biostratigraphy from the Dolomites and Greece. Earth and Planetary Science Letters 146, 107–120.
Muttoni, G., Garzanti, E., Alfonsi, L., Cirilli, S., Germani, D., Lowrie, W., 2001. Motion of Africa and Adria since the Permian: paleomagnetic and paleoclimatic constraints from northern Libya. Earth and Planetary Science Letters 192, 159–174.
Muttoni, G., Kent, D.V., Garzanti, E., Brack, P., Abrahamsen, N., Gaetani, M., 2003. Early Permian Pangea 'B' to Late Permian Pangea 'A'. Earth and Planetary Science Letters 215, 379–394.
Muttoni, G., Nicora, A., Brack, P., Kent, D.V., 2004. Anisian–Ladinian boundary chronology. Palaeogeography, Palaeoclimatology, Palaeoecology 208, 85–102.
Muttoni, G., Erba, E., Kent, D.V., Bachtadse, V., 2005. Mesozoic Alpine facies deposition as a result of past latitudinal plate motion. Nature 434, 59–63.
Muttoni, G., Gaetani, M., Kent, D.V., Sciunnach, D., Angiolini, L., Berra, F., Garzanti, E., Mattei, M., Zanchi, A., 2009. Opening of the Neo-Tethys Ocean and the Pangea B to Pangea A transformation during the Permian. GeoArabia 14, 17–48.
Muttoni, G., Kent, D.V., Jadoul, F., Olsen, P.E., Rigo, M., Galli, M.T., Nicora, A., 2010. Rhaetian magneto-biostratigraphy from the Southern Alps (Italy): constraints on Triassic chronology. Palaeogeography, Palaeoclimatology, Palaeoecology 285, 1–16.
Palencia-Ortas, A., Ruiz-Martinez, V., Villalain, J., Osete, M., Vegas, R., Touil, A., Hafid, A., McIntosh, G., Van Hinsbergen, D., Torsvik, T., 2011. A new 200 Ma paleomagnetic pole for Africa, and paleo-secular variation scatter from Central Atlantic Magmatic Province (CAMP) intrusives in Morocco (Ighrem and Foum Zguid dykes). Geophysical Journal International 185, 1220–1234.
Reilly, T., Raja, P., Mussett, A., Brock, A., 1976. The palaeomagnetism of Late Cenozoic volcanic rocks from Kenya and Tanzania. Geophysical Journal of the Royal Astronomical Society 45, 483–494.
Renne, P.R., Scott, G.R., Glen, J.M.G., Feinberg, J.M., 2002. Oriented inclusions of magnetite in clinopyroxene: source of stable remanent magnetization in gabbros of the Messum Complex, Namibia. Geochemistry, Geophysics, Geosystems 3, 1079.
Riisager, P., Knight, K.B., Baker, J.A., Ukstins Peate, I., Al-Kadasi, M., Al-Subbary, A., Renne, P.R., 2005. Paleomagnetism and $^{40}Ar/^{39}Ar$ geochronology of Yemeni Oligocene volcanics: implications for timing and duration of Afro-Arabian traps and geometry of the Oligocene paleomagnetic field. Earth and Planetary Science Letters 237, 647–672.
Rosenbaum, G., Lister, G.S., Duboz, C., 2004. The Mesozoic and Cenozoic motion of Adria (central Mediterranean): a review of constraints and limitations. Geodinamica Acta 17 (2), 125–139.
Satolli, S., Besse, J., Speranza, F., Calamita, F., 2007. The 125–150 Ma high-resolution Apparent Polar Wander Path for Adria from magnetostratigraphic sections in Umbria–Marche (Northern Apennines, Italy): timing and duration of the global Jurassic–Cretaceous hairpin turn. Earth and Planetary Science Letters 257, 329–342.
Satolli, S., Besse, J., Calamita, F., 2008. Paleomagnetism of Aptian–Albian sections from the Northern Apennines (Italy): implications for the 150–100 Ma apparent polar wander of Adria and Africa. Earth and Planetary Science Letters 276, 115–128.
Schaltegger, U., Brack, P., 2007. Crustal-scale magmatic systems during intracontinental strike-slip tectonics: U, Pb and Hf isotopic constraints from Permian magmatic rocks of the Southern Alps. International Journal of Earth Sciences 96, 1131–1151.
Schneider, D.A., Kent, D.V., 1990. Testing models of the Tertiary paleomagnetic field. Earth and Planetary Science Letters 101, 260–271.
Scholger, R., Mauritsch, H.J., Brandner, R., 2000. Permian–Triassic boundary magnetostratigraphy from the Southern Alps (Italy). Earth and Planetary Science Letters 176, 495–508.
Schult, A., 1973. Palaeomagnetism of Upper Cretaceous volcanic rocks in Sicily. Earth and Planetary Science Letters 19, 97–100.
Schult, A., Soffel, H., 1973. Palaeomagnetism of Tertiary basalts from Libya. Geophysical Journal of the Royal Astronomical Society 32, 373–380.
Sichler, J.L., Olivet, J.M., Auzende, H., Jonquet, H., Bonnin, J., Bonifay, A., 1980. Mobility of Morocco. Canadian Journal of Earth Sciences 17, 1546–1558.
Silva, P.F., Henry, B., Marques, F.O., Mateus, A., Madureira, P., Lourenco, N., Miranda, J.M., 2006. Variation of magnetic properties in sedimentary rocks hosting the Foum Zguid dyke (southern Morocco): combined effects of re-crystallization and Fe-metasomatism. Earth and Planetary Science Letters 241, 978–992.
Speranza, F., Sagnotti, L., Mattei, M., 1997. Tectonics of the Umbria–Marche–Romagna arc (central-northern Apennines, Italy): new paleomagnetic constraints. Journal of Geophysical Research 102, 3153–3166.
Speranza, F., Minelli, L., Pignatelli, A., Chiappini, M., 2012. The Ionian Sea: the oldest in-situ ocean fragment of the world? Journal of Geophysical Research 117, B12101. http://dx.doi.org/10.1029/2012JB009475.
Storetvedt, K., Vage, H.M., Aase, S., Lovlie, R., 1979. Palaeomagnetism and the early magmatic history of Fuerteventura (Canary Islands). Journal of Geophysics 46, 319–334.
Steinberger, B., Torsvik, T.H., 2008. Absolute plate motions and true polar wander in the absence of hotspot tracks. Nature 452, 620–623. http://dx.doi.org/10.1038/nature06824.
Tauxe, L., Besse, J., La Brecque, J.L., 1983. Palaeolatitudes from DSDP Leg 73 sediment cores; implications for the apparent polar wander path for Africa during the late Mesozoic and Cenozoic. Geophysical Journal of the Royal Astronomical Society 73, 315–324.
Tauxe, L., Kent, D.V., 1984. Properties of a detrital remanence carried by haematite from study of modern river deposits and laboratory redeposition experiments. Geophysical Journal of the Royal Astronomical Society 77, 543–561.
Tauxe, L., Kent, D.V., 2004. A simplified statistical model for the geomagnetic field and the detection of shallow bias in palaeomagnetic inclinations: was the ancient magnetic field dipolar? In: Channell, J.E.T., Kent, D.V., Lowrie, W., Meert, J.G. (Eds.), Timescales of the Palaeomagnetic Field, Geophys. Monogr. Ser., 145. American Geophysical Union, pp. 101–145.
Tauxe, L., Kodama, K.P., Kent, D.V., 2008. Testing corrections for paleomagnetic inclination error in sedimentary rocks: a comparative approach. Physics of the Earth and Planetary Interiors 169, 152–165.
Tauxe, L., 2010. Essentials of Paleomagnetism. University of California Press, Berkeley.
Torsvik, T.H., Tucker, R.D., Ashwal, L.D., Eide, E.A., Rakotosolofo, N.A., de Wit, M.J., 1998. Late Cretaceous magmatism in Madagascar: palaeomagnetic evidence for a stationary Marion hotspot. Earth and Planetary Science Letters 164, 221–232.
Torsvik, T.H., Muller, R.D., Van der Voo, R., Steinberger, B., Gaina, C., 2008. Global plate motion frames: toward a unified model. Reviews of Geophysics 46, RG3004.
Torsvik, T.H., Van der Voo, R., Preeden, U., Mac Niocaill, C., Steinberger, B., Doubrovine, P.V., van Hinsbergen, D.J.J., Domeier, M., Gaina, C., Tohver, E., 2012. Phanerozoic polar wander, palaeogeography and dynamics. Earth-Science Reviews 114, 325–368.
Van der Voo, R., 1993. Paleomagnetism of the Atlantic, Tethys and Iapetus Oceans. Cambridge University Press, Cambridge.
Van Fossen, M.C., Kent, D.V., 1993. A palaeomagnetic study of 143 Ma kimberlite dikes in central New York State. Geophysical Journal International 113, 175–185.
Van Hilten, D., 1960. Geology and permian paleomagnetism of the Val-di-Non area W. Dolomites, N. Italy. Geologica Ultraiectina 5, 1–100.
Van Hilten, D., 1962. A deviating Permian pole from rocks in northern Italy. Geophysical Journal of the Royal Astronomical Society 6, 377–390.
Van Hilten, D., Zijderveld, J., 1966. Paleomagnetism and the Alpine tectonics of Eurasia U the magnetism of the Permian porphyries near Lugano (Northern Italy, Switzerland). Tectonophysics 3, 429–446.
Van Zijl, J.S.V., Graham, K.W.T., Hales, A.L., 1962. The paleomagnetism of the Stromberg lavas II. The behaviour of the magnetic field during a reversal. Geophysical Journal 7, 169–182.

Watkins, N., 1973. Palaeomagnetism of the Canary Islands and Madeira. Geophysical Journal of the Royal Astronomical Society 32, 249–267.
Westphal, M., Montigny, R., Thizat, R., Bardon, C., Bossert, A., Hamzeh, R., 1979. Paléomagnétisme et datation du volcanisme permien, triasique et crétacé du Maroc. Canadian Journal of Earth Sciences 16, 2150–2163.
Wiedenmayer, F., 1980. Die Ammoniten der mediterranean provinz in Pliensbachian und im unteren Toarcian aufgrund neuer Untersuchungen im Generoso–Becken (Lombardische Alpen). Denkschriften der Schweizerischen Naturforschenden Gesellschaft 93, 1–260.
Zijderveld, J.D.A., De Jong, K.A., 1969. Paleomagnetism of some Late Paleozoic and Triassic rocks from the eastern Lombardic Alps. Geologie en Mijnbouw 48, 559–564.
Zijderveld, J.D.A., Hazeu, G.J.A., Nardin, M., Van der Voo, R., 1970. Shear in the Tethys and the Permian paleomagnetism in the Southern Alps, including new results. Tectonophysics 10, 639–661.